Quantifying the Contribution of Ocean Mesoscale Eddies to Low Oxygen Extreme Events.

JAMIE ATKINS

A dissertation submitted to the University of Bristol in accordance with the requirements of the degree of Master of Science by Research in the Faculty of Science.

School of Geographical Sciences

AUGUST 2021

Word count: 15,148

Abstract

Oceanic dissolved oxygen has declined in recent decades (ocean deoxygenation) and represents a major stressor on marine life and biogeochemistry. Yet, the future extent and distribution of oxygen decline in the global ocean is uncertain. Mesoscale eddies, which are abundant in the global ocean, have a potentially large influence on the redistribution of dissolved oxygen in low oxygen zones. However, eddies and their biogeochemical consequences are understudied owing to the difficulty in resolving these fine-scale features in coarse ocean climate model simulations. Moreover, adequately tracking eddy features, and isolating their biogeochemical signals through the water column is challenging. Here, a global physical-biogeochemical ocean model at eddy-permitting resolution is employed to conduct an eddy-oxygen census of features originating in and around four Eastern Boundary Upwelling Systems (EBUS), located adjacent to Oxygen Minimum Zones (OMZs). Eddies with a surface signature, of both cyclonic and anticyclonic nature, are tracked over the period 1992–2018, and their subsurface biogeochemical signatures are isolated. Strongly deoxygenating eddies are characterised and their contribution to low oxygen extreme events (< 1st percentile) is quantified. It is found that eddies, in particular cyclones, are associated with intense negative oxygen anomalies in all focus regions, likely due to the trapping of low oxygen source waters and potential oxygen depletion mechanisms across eddy lifetimes. For the first time, the enhanced frequency of low oxygen extreme events within an eddy relative to non-eddying locations in EBUS locations is demonstrated (consistently 2-7 times higher in eddies vs. non-eddying locations). Finally, results of this investigation also suggest that eddies have substantially contributed to low oxygen extreme events across large areas outside of the permanent OMZs over the past decades.

Acknowledgements

I would like to wholeheartedly thank my primary supervisor, Dr Oliver Andrews, for his expert guidance, support and encouragement throughout the thesis process. I would also like to thank Dr Dann Mitchell and Dr Ivy Frenger for their support as secondary supervisor and co-author to publication, respectively. We thank MERCATOR OCEAN and the Copernicus Marine Environment Monitoring Service for making FREEGLORYS2V4 and FREEBIORYS2V4 model data available, which are used to generate the research output, as well as the satellite observational product (previously AVISO+). We also thank Eric Oliver for providing eddy tracking code.

Thank you to my family and friends for their unwavering support. Finally, thank you Saskia, for her continual enthusiasm to go on stress-relieving cycles.

P.S. Thank you to the Orthopaedics team at Bristol Royal Infirmary for fixing my hand after the only not-so-stress-relieving cycle.

P.P.S. Saskia not involved in the particular ride in question.

Author's Declaration

I declare that the work in this dissertation was carried out in accordance with the requirements of the University's Regulations and Code of Practice for Research Degree Programmes and that it has not been submitted for any other academic award. Except where indicated by specific reference in the text, the work is the candidate's own work. Work done in collaboration with, or with the assistance of, others, is indicated as such. Any views expressed in the dissertation are those of the author.

SIGNED:

DATE:

Table of Contents

Thesis Preamble **1**

1 – Introduction **1**

2 – Literature Review **3**

2.1 – Ocean deoxygenation, Eastern Boundary Upwelling Systems, and eddies 3

2.2 – Eddy formation and physical characteristics 6

2.3 – Low oxygen eddies 7

2.3.1 – Eddy physical-biogeochemical mechanisms 7

2.3.2 – Regional variation in eddy physical-biogeochemical mechanisms 12

2.4 – Eddy tracking strategies 12

2.4.1 – Modelling eddies 12

2.4.2 – Eddy identification and autonomous tracking 13

2.5 – Eddies in future climate 15

3 – Data and Methods **16**

3.1 – Eddy-permitting ocean model simulations 17

3.2 – Data analysis framework 17

3.2.1 – Eddy-oxygen census 17

3.2.2 – Eddy property calculations 20

3.2.3 – Eddy low oxygen extreme events methodology 21

3.3 – Ocean model validation 22

4 – Results **25**

4.1 – Eddy-oxygen profiles 26

4.2 – Characterisation of low oxygen eddies 29

4.3 – Eddy low oxygen extreme events 31

5 – Discussion **34**

5.1 – Eddy-oxygen profiles 34

5.2 – Characterisation of low oxygen eddies 35

5.3 – Eddy low oxygen extreme events 36

6 – Conclusions **37**

6.1 – Eddies and low oxygen extreme events 37

6.2 – Key limitations 39

References **40**

List of Tables

Table		Page
3.1	Number of eddies (total CEs and ACEs) over the period 1993-2018 in FREEGLORYS2V4 (model) and observations (obs) for the common period of 1993-2018.	23

List of Figures

Figure		Page
2.1	Illustrations of a) eddy trapping and b) eddy pumping mechanisms in typical northern hemisphere cyclonic eddy water columns, as examples of lateral and vertical transport mechanisms respectively. Red arrows denote rotation of the eddy, whilst white lines show isopycnal layers. Illustrations created by the author.	9
3.1	Tracks of CEs (blue) and ACEs (red) in focus regions (marked by black boxes) across the period 1992-2018, which exceed a 4-week lifetime and originate in low oxygen waters (< 200 mmol m^{-3} depth averaged over ≈ 50–200 m). This constrained dataset does not match the datasets used in subsequent sections of this work and is shown only to illustrate the tracking procedure. Background shows climatological oxygen concentration at ≈ 200 m depth [mmol m^{-3}]. Initial detection points of eddies are indicated by white dots.	18
3.2	(a) CE and (b) ACE counts per year in focus regions (marked by boxes), which exceed a 1-week lifetime, across the simulation period 1992–2018, in 1°x1° bins. Background contours show climatological oxygen concentration at ≈ 200 m depth [mmol m^{-3}].	20
3.3	Frequency distributions of eddy a) lifetime, b) radius, c) area, and d) amplitude in eddies tracked (those which exceed 1-week lifetimes, both CEs and ACEs) in model simulations (blue line; FREEGLORYS2V4) and observations (black line; CMEMS), across the period 1993-2018. All eddies tracked in the four focus regions of this study are composited to form a singular EBUS distribution for each variable.	24
3.4	a) FREEBIORYS2V4 modelled mean oxygen concentrations (across 1993-2018), b) WOA2018 observed mean oxygen concentrations (across 1955-2018), and c) difference between mean oxygen concentrations in WOA2018 and model simulation (observations – model), at ≈ 200 m depth.	25
4.1	Frequency distributions of dissolved oxygen concentration (5 mmol m^{-3} bins) beneath the centroids of CEs (red line), ACEs (blue line) and regional climatology (black line), at depth levels within the range ≈ 50-200 m, in focus regions. CEs and ACEs are tracked over the period 1992-2018 and are constrained by those which originate in low oxygen waters (< 200 mmol m^{-3}). Light red shading represents approximate hypoxic concentrations (< 60 mmol m-3), darker red shading shows approximate suboxic concentrations (< 5 mmol m^{-3}).	26
4.2	Distributions of eddy oxygen anomaly (10 mmol m^{-3} bins) at depth levels within the range ≈ 50-200 m beneath the centroids of CEs (blue) and ACEs (red) which originate in low oxygen waters (< 200 mmol m^{-3}) in focus regions, tracked over the period 1992-2018. Grey bar subplots show difference between CE and ACE distributions (i.e. difference between red and blue lines) in terms of percentage point (pp) difference within each oxygen anomaly bin.	27
4.3	Composite oxygen (blue for CEs, red for ACEs) and (-1)*AOU (purple for CEs, green for ACEs; mmol m^{-3}) anomaly depth profiles beneath centroids of CEs and ACEs which originate in low oxygen waters (< 200 mmol m^{-3}) in focus regions, tracked over the period 1992–2018. Anomalies expressed relative to a non-eddying background field. Solid lines are mean values of all eddies at each model depth. Shading represents ± 1 standard deviations.	28

Figure		Page
4.4	Composite O_2sat anomaly depth profiles beneath the centroids of CEs (brown) and ACEs (yellow) which originate in low oxygen waters (< 200 mmol m^{-3}) in focus regions, tracked over the period 1992-2018. Anomalies expressed relative to a non-eddying background field. Solid lines are mean values of all eddies at each model depth, thereby forming a composite depth profile. Shading represents ± 1 standard deviations.	29
4.5	Surface radius vs. oxygen anomaly of CEs (blue) and ACEs (red) which originate in low oxygen waters (< 200 mmol m^{-3}) in each EBUS focus region, tracked over the period 1992-2018. For each eddy, oxygen anomaly values are depth averaged over ≈ 50-200 m, and temporally averaged across the eddy lifetime. Surface radius values are averaged across eddy lifetime. Solid lines show ordinary least squares regression, and text shows accompanying regression statistics.	30
4.6	(a) Eddy amplitude, (b) rotational velocity and (c) nonlinearity vs. oxygen anomaly in CEs (blue) and ACEs (red) which originate in low oxygen waters (< 200 mmol m-3), tracked over the period 1992-2018. CE and ACE data from each focus region is combined to produce a global EBUS dataset for each variable. For each eddy, oxygen anomaly values are depth averaged over ≈ 50-200 m, and temporally averaged over the eddy lifetime. Amplitude, rotational velocity and nonlinearity values are averaged over the eddy lifetime. Solid lines show ordinary least squares regression, and accompanying text shows regression statistics.	31
4.7	(a) Frequency (percentage of total CEs/ACEs/non-eddies which experience low oxygen extreme events) and (b) mean intensity (minimum oxygen concentration within CE/ACE/non-eddy low oxygen extreme events across 0-300 m depth beneath the eddy centroid) of CE (blue bars), ACE (red bars) and non-eddy (grey bars) oxygen extreme events in focus regions, across the period 1992-2018. Error bars show ± 1 standard deviation. Eddies in permanent OMZs are not shown.	32
4.8	Percentage contribution (% of total number of extreme event days) of low oxygen extreme event days by CEs (blue shading) and ACEs (red shading) in focus regions outside permanent OMZs, across the simulation period 1992-2018, in 1°x1° bins. Only values exceeding 1% are shown. In bins where CEs and ACEs both exceed 1%, the higher value is plotted and stippling marks such locations. Contours show climatological oxygen concentrations (mmol m^{-3}).	33

Thesis Preamble

This work is based on a manuscript submitted to Geophysical Research Letters: 'Atkins, J., Andrews, O. and Frenger, I. 2021. Quantifying the Contribution of Ocean Mesoscale Eddies to Oxygen Extreme Events. In Review.'. The Introduction, Data and Methods, Results, Discussion, and Conclusions sections of this thesis share similarities to the content of the manuscript submission, though they are largely extended in the thesis. The Title of the work is shared between both documents. The Literature Review section in the thesis is not included in the upcoming manuscript submission, and includes an expanded background section compared to the content of the manuscript and thesis Introduction sections. Versions of figures similar to Figures 3.2, 4.3, 4.7, and 4.8 in the thesis are common between the thesis and the main text of the manuscript submission, whilst Figures 3.3, 3.4, and 4.4 are common between the thesis and manuscript Supplementary Information. Author collaboration with Andrews, O. and Frenger, I. for the manuscript includes supervisory and conceptualisation help, and review of written work. The analysis, write up, and data processing were carried out by the lead author.

1 – Introduction

Dissolved oxygen (henceforth "oxygen") in the global ocean has been in unnatural decline over the last 50 years – a phenomenon labelled 'ocean deoxygenation' – and tropical oxygen minimum zones (OMZs) have expanded (Stramma *et al.*, 2012b). The impacts of low oxygen waters are grave for marine life. Below the threshold of 'hypoxia' (< 60 mmol m^{-3}; Gray *et al.*, 2002), the physiology of a spectrum of taxa, including fisheries, are negatively impacted by deoxygenation (Vaquer-Sunyer and Duarte, 2008; Keeling *et al.*, 2010). Subsequent effects may include, for example, habitat compression of tropical pelagic fish (e.g. Stramma *et al.*, 2012b). Meanwhile at 'suboxic' levels (< 5 mmol m^{-3}; Keeling *et al.*, 2010), ocean biogeochemistry is impacted, for example with some bacteria beginning to favour denitrification which is associated with the release of a potent greenhouse gas, namely nitrous oxide, therefore potentially contributing to global warming (Gruber, 2008; Codispoti, 2010). A problem troubling the deoxygenation research community, however, is the inability of the current generation of Earth System Models from phase 5 of the Coupled Model Intercomparison Project (CMIP5) to adequately reproduce the mean state (Cabré *et al.*, 2015) and historical changes in tropical OMZ regions (Stramma *et al.*, 2012a; Andrews *et al.*, 2013; Oschlies *et al.*, 2018). Projections for the future of ocean deoxygenation in the tropics are, therefore, uncertain and lacking in consensus (Bopp *et al.*, 2013, 2017). This mismatch between simulation and observation is suggested to arise because of important physical processes that are missing within the current generation of CMIP5 models (e.g. Stramma *et al.*, 2012a). Such processes include mesoscale circulation features, such as mesoscale ocean eddies (henceforth "eddies"), which may act to redistribute oxygen in OMZ regions (e.g. Hahn *et al.*, 2014).

However, it is not yet clear if representing the oceanic mesoscale is fundamental to correctly modelling oxygen trends.

Eddies are characterised by intense rotation, are formed via flow instabilities in ocean currents, and exhibit prevailing westward propagation post-genesis (Chelton *et al.*, 2011b). However, at the mesoscale (i.e. on the order of 100 km spatial scale), eddies are not explicitly resolved in the existing generation of coarse resolution CMIP5 models (Stramma *et al.*, 2012a). Eddies play an important role in the spatiotemporal distribution of ocean tracer signals via a series of physical and biogeochemical mechanisms in cyclonic (CEs) and anticyclonic eddies (ACEs) (McGillicuddy, 2016). Mechanisms include lateral transport processes, such as 'eddy trapping' where the strong rotation of an eddy is considered capable of isolating water masses within the eddy structure (Chelton *et al.*, 2011b). Low oxygen source waters in OMZ regions may therefore be trapped by eddies forming in these locations before propagating westward, as evidenced by observations of low oxygen values in CEs and intrathermocline eddies forming in the eastern section of the North Eastern Pacific (Schütte *et al.*, 2016b). Furthermore, eddies may impact oxygen consumption via locally modulating export of organic matter. Chelton *et al.* (2011a) and Gaube *et al.* (2014) show regional variability in near-surface chlorophyll is associated with the movement of westward propagating eddies, which may be due to lateral transport of nutrients or organic matter. Additional mechanisms include local impacts on productivity within eddies via vertical transport of nutrients from below in the water column, which has subsequent effects on oxygen consumption. Examples of physical processes associated with vertical transport in eddies include 'eddy pumping' (Falkowski *et al.*, 1991) and 'eddy-induced Ekman pumping' (e.g. Gaube *et al.*, 2015). With these physical-biogeochemical processes in mind, I postulate that eddies have the potential to modulate subsurface oxygen in and around OMZ regions.

Eastern Boundary Upwelling Systems (EBUS) are zones of high biological productivity and energetic ocean currents, which produce large numbers of eddies (Mahadevan, 2014). Eddies originating in EBUS locations tend to be longer lived, which allows them to propagate far offshore and into the subtropical gyres (Chelton *et al.*, 2011b; Lovecchio *et al.*, 2018). Therefore, given the long lifetimes, this may allow eddies in these regions to transport biogeochemical signatures across large distances and oxygen gradients (e.g. from OMZ waters to the otherwise more oxygenated open ocean), as well as allow oxygen consumption to accumulate, provided eddies are well isolated. Low oxygen conditions in eddies, particularly CEs, are well documented in observational studies for the Atlantic (Karstensen *et al.*, 2015; Löscher *et al.*, 2015; Schütte *et al.*, 2016b) and Pacific EBUS regions (Stramma *et al.*, 2013; Arévalo-Martínez *et al.*, 2016; Czeschel *et al.*, 2018). Moreover, the influence of subsurface intensified anticylonic 'puddies' (poleward undercurrent eddies) on the redistribution of low oxygen conditions from EBUS into the subtropical gyres has been described by Frenger *et al.* (2018). Localised extremely low oxygen conditions (< 1–10 mmol m^{-3}) have also been observed in "dead zone" eddies of the eastern tropical North Atlantic (Karstensen *et al.*, 2015; Schütte *et al.*, 2016b), with

significant implications for ecosystems (e.g. Hauss *et al.*, 2016) and marine N_2O production (Grundle *et al.*, 2017).

This study presents a first model-based assessment of the influence of eddies, that are detectable at the ocean surface, in and around Atlantic and Pacific EBUS regions on the development of low oxygen conditions and extreme events. There currently exists no such study, in part due to the limited availability of simulations of sufficient resolution to adequately resolve the mesoscale, as well as the difficulty in autonomously tracking eddies and associating them with the accompanying simulated biogeochemistry. A model's ability to resolve the mesoscale at different latitudes is governed largely by the ratio between the horizontal grid spacing and the latitude-dependent Rossby radius of deformation (Hallberg, 2013; Moreton *et al.*, 2020). Models that are of high enough resolution to resolve the mesoscale at low- and mid-latitudes are commonly labelled "eddy permitting/present" (loosely defined as a minimum 1/4° horizontal grid-spacing), whilst "eddy resolving/rich" models (1/12° horizontal spacing) are thought to be capable of resolving features at most latitudes (Fox-Kemper *et al.*, 2014). To that end, this investigation employs an eddy-permitting resolution model, including physical and biogeochemical processes, to create a 'complete dataset' eddy-oxygen census over a multi-decadal time-period. Furthermore, an autonomous eddy tracking algorithm is employed to identify eddies in space-time from sea surface height (SSH) anomaly fields in four key focus regions, including – and expanding westward of – the globe's four predominant Eastern Boundary Upwelling Systems (EBUS). They are henceforth referred to as the North Eastern Atlantic (NEA), South Eastern Atlantic (SEA), North Eastern Pacific (NEP), and South Eastern Pacific (SEP) (see Figure 3.1 black boxes for indication of locations). These regions mirror those in other eddy-oxygen studies (e.g. Frenger *et al.*, 2018) and are chosen primarily because they are proximal to important OMZs, which are regions suggested to be sensitive to warming and contain ecosystem-relevant low oxygen waters (e.g. Stramma *et al.*, 2012b), as well as being where current models are most lacking in skill. In addition, they contain strong ocean currents from which many eddies spin off (Mahadevan, 2014). This investigation seeks to address three primary objectives: i) to produce the first, comprehensive characterisation of surface detectable eddy oxygen profiles in all focus regions, ii) to assess the driving characteristics of eddy oxygen responses; and iii) to quantify the contribution of eddies to the extremely low oxygen (< 1st percentile) in the EBUS regions.

2 – Literature Review

2.1 – *Ocean deoxygenation, Eastern Boundary Upwelling Systems, and eddies*

As stated in the Fifth Assessment Report of the Intergovernmental Panel on Climate Change (IPCC), the global inventory of dissolved oxygen in the ocean has been in unnatural decline for the past approximately 50 years – a process labelled 'ocean deoxygenation' – likely associated with anthropogenic warming (Rhein *et al.*,

2013). Oxygen Minimum Zones (OMZs) are naturally occurring in the global ocean (Paulmier and Ruiz-Pino, 2009), though these have likely expanded as part of the ocean deoxygenation phenomenon (Stramma *et al.*, 2012a). Generally, ocean deoxygenation has likely been occurring in response to an ocean warming trend (Keeling *et al.*, 2010). That is, the solubility of oxygen in warmer ocean waters is reduced and there is reduced ventilation/increased stratification, thereby limiting the transfer of oxygen between ocean layers (Bopp *et al.*, 2017). Ocean deoxygenation is of concern due to the grave consequences it may pose for marine life and biogeochemistry. Thresholds of low oxygen conditions are recognised in the literature as having distinct effects on marine life. At high trophic levels, for example fish and crustacea, the impact of thresholds of low oxygen is species dependent (Karstensen *et al.*, 2015). However, *hypoxic* concentrations, (below approximately 60 mmol m^{-3}; Gray *et al.*, 2002), are generally lethal for most taxa (Keeling *et al.*, 2010). Additionally, open ocean oxygen concentrations approaching these values can result in the suppression of available habitat for pelagic fish. For example, blue marlin have experienced an approximately 15% habitat suppression over the period 1960-2010 according to Stramma *et al.* (2012b). In addition, there is evidence in Diaz and Rosenberg (2008) of mass mortality of fish as oxygen concentrations decline in the ocean. Moreover, it is suggested that at *suboxic* concentrations (of approximately 5 mmol m^{-3} and below; Keeling *et al.*, 2010), ocean biogeochemistry begins to be significantly impacted. For example, organisms may begin to favour denitrification in these conditions, thereby releasing nitrous oxide gas, a powerful greenhouse gas, which may potentially further contribute to climate change (Gruber, 2008; Codispoti, 2010; Naqvi *et al.*, 2010; Arévalo-Martínez *et al.*, 2015). Studies such as Farías *et al.* (2009) demonstrate the role of OMZs as sources of nitrous oxide gas to the atmosphere.

Given the close association between historical ocean deoxygenation and global warming trends, it is likely that a continued climate warming trend in the future will correspondingly exacerbate future ocean deoxygenation (Bopp *et al.*, 2013). However, significant uncertainties in model future projections exist, especially so in subsurface tropical regions which contain the main global OMZs (Bopp *et al.*, 2017). There are severe mismatches between the current generation of Earth System Models from phase 5 of the Coupled Model Intercomparison Project (CMIP5) and historical observations of ocean deoxygenation trends (Stramma *et al.*, 2012a), signalling a lack of skill in these simulations. Cabré *et al.* (2015) show that the models are generally unable to adequately reproduce the mean state of OMZ regions. In addition, it is well demonstrated that historical changes in the tropical OMZ regions are also poorly simulated (Stramma *et al.*, 2012a; Andrews *et al.*, 2013; Oschlies *et al.*, 2018).

In general, locations of OMZs – the very lowest values of oxygen in the oceans – are dictated by characteristics of oceanic biogeochemical cycling and physical ocean ventilation. The eastern tropical regions of the Pacific and Atlantic oceans represent notable locations of sluggish mixing/ventilation and high productivity where major OMZs exist at approximately 100-900 m depth (Karstensen *et al.*, 2008). Eastern Boundary Upwelling

Systems (EBUS) are unique regions of interest, which lie inside the eastern/coastal margins of the Pacific and Atlantic OMZs. Alongshore winds in these areas drive an offshore mean flow in EBUS, which generates upwelling of deeper, colder and nutrient-rich waters. Once drawn up into the euphotic zone, this creates highly productive surface waters (Mahadevan, 2014). Owing to high rates of productivity, this enhances oxygen consumption and therefore depletes the oxygen inventory. To compound this, EBUS regions experience weak ventilation of intermediate waters, which results in the maintenance of low oxygen waters (Karstensen *et al.*, 2008). There exist four major EBUS regions globally, which sit within the vast Pacific and Atlantic OMZs, namely the North Eastern Atlantic (NEA), South Eastern Atlantic (SEA), North Eastern Pacific (NEP), and South Eastern Pacific (SEP).

The alongshore currents in EBUS are high energy and unstable. Therefore, they are prone to casting eddies off into the open ocean waters (Mahadevan, 2014). Owing to the ability of eddies to modulate and transport the biogeochemically anomalous waters (including low oxygen anomalies) of the EBUS regions with them offshore, these features are frequently discussed in the literature with regards to their role in the redistribution of biogeochemical conditions (to be further discussed in subsequent sections). Chelton *et al.* (2011b) show that eddies in and around EBUS regions are often long-lived, thereby allowing for long distance propagation across oxygen gradients into the open ocean as well the accumulation of oxygen consumption via biological mechanisms (Lovecchio *et al.*, 2018). Studies have been conducted in and around EBUS with a focus on low oxygen conditions within the eddies (e.g. Karstensen *et al.*, 2015; Fiedler *et al.*, 2016; Schütte *et al.*, 2016b; Czeschel *et al.*, 2018). Broadly, these observational studies find low oxygen conditions within eddies, attributable to the trapping of the OMZ waters in which they originate and/or the subsequent modulation of oxygen via their internal dynamics. Formation of eddies in and around EBUS regions and their mechanisms modulating oxygen will be discussed in greater detail from Section 2.2 onwards.

As suggested by Stramma *et al.* (2012a), a potential explanation for the discrepancy between models and observations in reproducing historical ocean deoxygenation in OMZs, as mentioned previously, may be the inability of the models to resolve mesoscale ocean eddies, owing to limitations in spatial resolution in the current generation of ocean models (see Section 2.4.1). Eddies' potential ability to redistribute oxygen may also, therefore, be a missing process which could add to the skill of simulations. Despite a growing interest in low oxygen conditions in eddies in and around EBUS regions in observational studies, there exist very few studies which gather a 'complete' modelled dataset perspective of the eddies in and around EBUS regions. Therefore, their role as localised low oxygen environments with significant consequences for marine life and biogeochemistry, as well as their up-until-now unquantified role in redistributing oxygen in and around EBUS regions, remains understudied. An investigation by Frenger *et al*. (2018) is one study which highlights the ability of subsurface eddies to spin off EBUS poleward undercurrents into the open ocean and carry a low oxygen signal in tow for several months.

2.2 – *Eddy formation and physical characteristics*

Global observations show that the ocean mesoscale field is dominated westward propagating flows. This westward prevalence was originally attributed entirely to the dynamics of linear Rossby waves, which are planetary waves occurring due to the rotation of the Earth (Chelton *et al.*, 2011b; Zhang *et al.*, 2016). However, upon close investigation, discrepancy is apparent, outside of tropical latitudes, when observed westward propagation speeds are compared to the speeds commonly associated with Rossby waves (Rossby and Collaborators, 1939; Chelton and Schlax, 1996). The advent of high-resolution ocean data has given rise to the notion that the prevailing westward propagation of mesoscale features is dominated by vortex-like eddies (localised flows with approximately circular motion and concentrated vorticity; McWilliams, 2006) as opposed to linear Rossby waves (Chelton *et al.*, 2007, 2011b). This prevalence of eddies is significant as it is precisely the vorticity of these features that allows for the development of unique characteristics with biogeochemical consequences for the oceans (McGillicuddy, 2016).

There are several mechanisms for eddy generation including, for example, the interaction between large-scale ocean circulations with landmasses and topographical features, but predominantly they form via instabilities in the main body of a large ocean current (Arístegui *et al.*, 1994; Chaigneau *et al.*, 2009; Djakouré *et al.*, 2014; Müller, 2017; Aguedjou *et al.*, 2019). There are two primary forms of instability that stimulate the formation and longevity of eddies – namely barotropic and baroclinic instabilities. The emergence of an eddy from a barotropic flow – a flow with a reliance on pressure gradient only – occurs due to an instability in the shear flow where even a small perturbation can transform kinetic energy to turbulent energy, thereby amplifying and maintaining coherent structures and contributing to their longevity (McWilliams, 2006; Oliver *et al.*, 2015; Müller, 2017). By contrast, baroclinic instabilities arise in fluids whose density is dependent on both temperature and pressure, unlike solely pressure in barotropic flows. This is the most common form flow instability and is largely responsible for weather and eddy kinetic energy patterns in the atmosphere and oceans respectively (Olbers *et al.*, 2012; Vallis, 2017). Potential energy in a mean flow, in the form of a temperature gradient, can lead to turbulent flow to form an eddy in the ocean (Müller, 2017; Vallis, 2017). The Coriolis force acts upon the turbulences to spin water masses and create vortices (Kostianoy and Belkin, 1989). Eddies subsequently propagate westward into the open ocean via Rossby wave dynamics and specific basin-scale circulations (Schütte *et al.*, 2016a).

Eddies are classified into different types based on their direction of rotation – cyclonic eddies (CE) and anticyclonic eddies (ACE) – with the different eddy types resulting in different physical and biogeochemical characteristics (Chelton *et al.*, 2011b; Everett *et al.*, 2012; Czeschel *et al.*, 2018; Gaube *et al.*, 2019). Subject to the Coriolis force, a northern hemisphere CE rotates anticlockwise and a southern hemisphere CE clockwise, and vice versa in the case of ACEs. In terms of sea surface height (SSH) field and sea surface

temperature (SST), CEs (ACEs) are associated with surface depressions (elevations) and cold (warm) cores (Rhines, 2001).

2.3 – *Low oxygen eddies*

Eddies are often discussed in the literature regarding their pivotal role in global ocean biogeochemical cycles. They have the ability to isolate the unique biogeochemical conditions of their source waters by their strong rotation, as well as modify their biogeochemical conditions via internal dynamics in and around the euphotic zone (Klein and Lapeyre, 2009; Chelton *et al.*, 2011b; McGillicuddy, 2016). Marine life/biogeochemical consequences of low oxygen waters are typically constrained to OMZ regions where oxygen concentrations are permanently low, but it is the biogeochemically anomalous conditions and long-range transport characteristics of eddies which mean they may form vehicles for spreading these consequences into otherwise more oxygenated extra-OMZ waters. A modelling study by Frenger *et al.* (2018) of subsurface poleward undercurrent eddies, discusses a phenomenon termed the 'cannonball' effect, whereby EBUS-origin subsurface eddies transport the biogeochemical characteristics of their source waters (e.g. OMZ conditions) to the open ocean, potentially redistributing and expanding the reach of OMZ-like conditions in the oceans. Furthermore, observational studies of low oxygen eddies originating in EBUS waters (e.g. Karstensen *et al.*, 2015; Fiedler *et al.*, 2016; Schütte *et al.*, 2016b; Czeschel *et al.*, 2018), similarly note the potential for eddies to tow their low oxygen signal into the otherwise more oxygenated open ocean.

To date, as part of the wider eddy biogeochemistry picture, there exists literature (to be discussed in the following sub-sections) examining various pathways by which eddies develop anomalous biogeochemical conditions. These include lateral and vertical transport processes, ranging from physical trapping of source waters to modulation of biological productivity and therefore oxygen consumption to temperature and stratification effects.

2.3.1 – *Eddy physical-biogeochemical mechanisms*

Many studies focus on near-surface chlorophyll (CHL) in the ocean to identify surface biogeochemical properties in terms of biological productivity. The regional variation in the relationship between SSH anomaly (indicative of eddy presence due to eddies' tendency to depress/elevate SSH) and CHL across the global ocean gives insight into the variety of mechanisms which can modulate biogeochemical conditions in both CEs and ACEs (Gaube *et al.*, 2014; McGillicuddy, 2016). Enhanced CHL is indicative of increased productivity, which subsequently promotes increased consumption of oxygen (Schütte *et al.*, 2016b). Thus, studies exploring CHL characteristics of eddies are useful for learning of the productivity mechanisms which may subsequently contribute to oxygen variability within eddies.

The first mechanisms to discuss concern lateral physical transport processes within eddies. Eddies are thought to be capable of *trapping* the source waters of their origin location owing to their physical dynamics and nonlinearity. That is, if rotational velocity (U) exceeds translational velocity (c), i.e. $U/c > 1$, eddies are deemed nonlinear. In a nonlinear physical state, internal waters are unable to pass through the boundary of the strongly rotating waters at the eddy circumference, thus inhibiting the exchange of water mass properties at the eddy boundary (Chelton *et al.*, 2011b). See Figure 2.1a for a simplified visual representation of the eddy trapping mechanism. As the rotational properties are maintained across an eddy's lifetime, and given the westward propagation nature of eddies, this results in 'pockets' of isolated water masses which may exhibit biogeochemical conditions foreign to the location at which they are observed once they travel away from their source waters (Frenger *et al.*, 2018). This effect is seen in observational studies of CHL in eddies (e.g. Menkes *et al.*, 2002; Moore *et al.*, 2007) which note the presence of enhanced CHL within open ocean eddies derived from their source waters. Moreover, Lovecchio *et al.* (2018) demonstrate the long range offshore transport of organic matter via initial trapping by eddies of productive EBUS origins. With regards to oxygen inventories within eddies, the isolation and propagation behaviours of eddies is important when the source waters are themselves low in oxygen. For example, eddies form in EBUS locations which lie within oxygen minimum zones (OMZs) (as discussed in section 2.1), thereby trapping these conditions within their boundaries. In-situ observational studies (e.g. Karstensen *et al.*, 2015; Schütte *et al.*, 2016b) present EBUS-origin eddies which exhibit oxygen concentrations foreign to the location at which they are observed in the more oxygenated open ocean. Similarly, Frenger *et al.* (2018) perform an EBUS-centric ocean-biogeochemical modelling study to demonstrate the anomalous oxygen conditions within sub-surface poleward undercurrent eddies originating from these regions. They attribute much of this characteristic to the coherence of the features which they study, thereby implying that they have preserved the biogeochemical characteristics of their source waters.

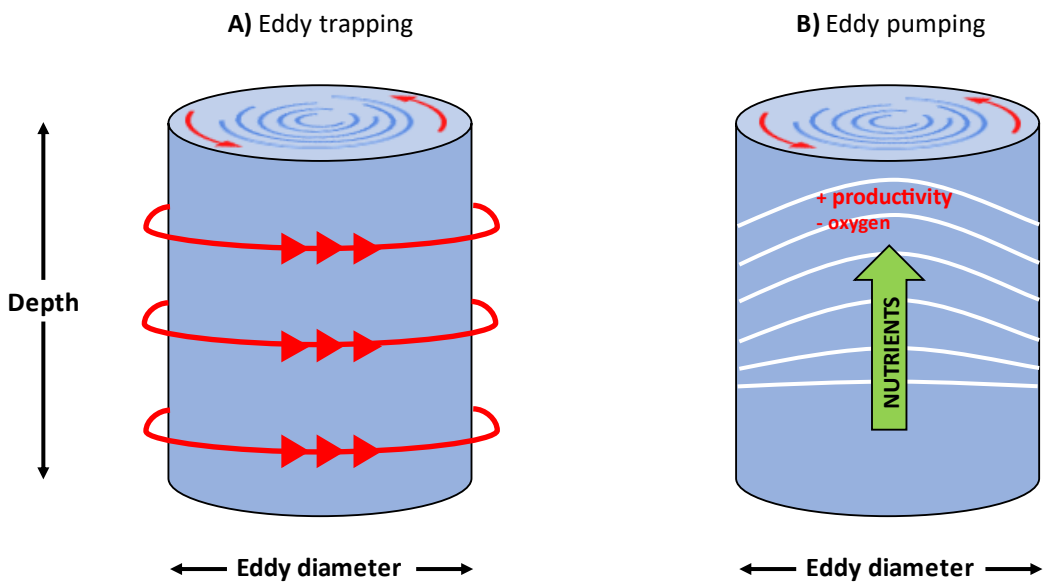

Figure 2.1 – Illustrations of a) eddy trapping and b) eddy pumping mechanisms in typical northern hemisphere cyclonic eddy water columns, as examples of lateral and vertical transport mechanisms respectively. Red arrows denote rotation of the eddy, whilst white lines show isopycnal layers. Illustrations created by the author.

In addition to the influence of water mass isolation effects, the inventory of oxygen within an eddy is suggested to be a balance between the trapping of waters and consumption of oxygen across the lifetime of the eddy (Frenger *et al.*, 2018). Observational studies hint at the potential for oxygen consumption within eddies. For example, Xiu and Chai (2020) demonstrate high Apparent Oxygen Utilisation (AOU) in CEs in the North Pacific, suggesting enhanced consumption. The first mechanism which may promote the consumption of oxygen in eddies is the lateral *eddy stirring* effect. The rotational forces of an eddy are able to perturb CHL distributions within an eddy by azimuthal advection to the extent where positive/negative anomalies can form in opposite quarters of the eddy dependent on the direction of rotation (McGillicuddy, 2016). Chelton *et al.* (2011a) investigate the eddy stirring phenomenon and cite it as a key mechanism for the manifestation of dipoles of CHL in eddies in the South Pacific.

Additional mechanisms thought capable of modulating productivity and consumption within eddies broadly all concern physical vertical transport within eddies. *Eddy pumping,* has long been acknowledged as a dominant mechanism in stimulating enhanced consumption within eddies (Falkowski *et al.*, 1991), but demonstrates an opposing effect in CEs and ACEs. The upward doming of isopycnals in CEs causes upwelling of nutrient-rich waters from depth, whilst the downward doming of isopycnals in ACEs leads to downwelling in the eddy centre. CE upwelling triggers enhanced productivity in the euphotic zone at the centre of the eddy, whilst there is an opposite depression of productivity at the centres of ACEs (Klein and Lapeyre, 2009; McGillicuddy, 2016). In the upwelling case of CEs, the subsequent respiration of increased organic matter then depletes the oxygen inventory within eddy waters (Fiedler *et al.*, 2016). Furthermore, eddy dynamics encourage complete utilisation of upwelled nutrients in CEs once transported into the euphotic zone. The

trapping of waters by the eddy rotation allows for the build-up of biomass in the eddy centre until all nutrients are spent (McGillicuddy, 2016). See Figure 2.1b for a simplified visual representation of the eddy pumping mechanism. Evidence for the eddy pumping mechanism is presented by Gaube *et al.* (2014) who show distinct monopoles of positive and negative CHL anomalies in CEs and ACEs, respectively, in the Gulf Stream region – consistent with the eddy pumping framework. However, it is difficult to assess whether the monopoles arise primarily due to eddy trapping or eddy pumping. Anomalies demonstrated upon initial detection suggests eddy trapping, whilst a subtle trend in strengthening anomalies also points towards eddy pumping as playing a role in enhancing productivity and consumption across the lifetime of an eddy (Gaube *et al.*, 2014; McGillicuddy, 2016).

Whilst the eddy pumping scheme explains enhanced CHL and depletion of oxygen within CEs well, it does not explain observations of enhanced CHL in ACEs (Greenwood *et al.*, 2007; Waite *et al.*, 2007; Gaube *et al.*, 2013; Dufois *et al.*, 2016). As such, the eddy pumping mechanism cannot be considered the sole possible explanation for increased productivity and consumption within eddies of all types. Instead, whilst the eddy pumping paradigm may remain significant in the case of CEs, there exist additional eddy vertical transport mechanisms which may enhance productivity and consumption within ACEs under certain scenarios. Indeed, under these regimes, some studies propose that ACEs are equally, if not more productive than their CE counterparts within major oceanic subtropical gyres (Dufois *et al.*, 2016; McGillicuddy, 2016; He *et al.*, 2017). The first of these mechanisms concerns the modulation of mixed layer depth (MLD) in eddies. Gaube *et al*. (2019) find that, on a global scale through satellite and autonomous float observations, ACEs deepen the MLD whilst CEs shoal it, with the magnitude of these MLD changes being largest in the winter months. Further, Dufois *et al.* (2014, 2016) argue that summer stratification is weaker in ACEs, which allows for deeper mixing in the winter and increased vertical flux of nutrients, thereby supporting CHL and productivity enhancement.

He *et al*. (2017) study satellite derived CHL observations within ACEs and make the case for a combined effect of winter mixing and eddy-Ekman vertical pumping. Eddy-Ekman related vertical movement concerns the interaction between mesoscale variability and wind, and the potential resultant upwelling of nutrients in ACEs which promote productivity. This process can come about by three different conditions. The first of which involves generalised Ekman divergence whereby the application of wind stress to eddy currents can create dipoles of upwelling and downwelling dependent on the wind direction and eddy vorticity sign (Flierl and McGillicuddy, 2002; McGillicuddy, 2016). Second, there is a sea surface temperature feedback whereby cooler waters stabilise the marine atmospheric boundary layer whilst warmer waters destabilise it. This has the resultant effect of either *i*) decoupling the above winds and decreasing surface wind speeds over cooler waters, or *ii*) decreasing vertical shear and therefore increasing surface wind speeds over warmer waters. Wind stress (curl) is thus altered over these waters which subsequently impacts Ekman pumping (Chelton *et*

al., 2004; Gaube *et al.*, 2015; McGillicuddy, 2016). Lastly, where the surface currents on the side of an eddy go against (along) the direction of the wind, there is an increase (decrease) in the wind stress of the respective side. Then, in the core of an ACE there is resultant eddy-induced Ekman suction (upwelling), and Ekman pumping (downwelling) in a CE (McGillicuddy, 2016). Gaube *et al.* (2015) assess the relative importance of all three eddy-Ekman related vertical transport mechanisms and find that in general the SST effect is less pronounced than the other two processes.

Studies discuss the case of the tendency for positive (negative) anomalies of CHL in ACEs (CEs) in the South Indian Ocean (e.g. Dufois *et al.*, 2014; Gaube *et al.*, 2014) and South-Eastern Pacific (e.g. He *et al.*, 2016). Here, the eddy-Ekman related vertical transport model is suggested to be a key mechanism at play. Whilst time series analysis in the Gaube *et al.* (2014) study show anomalies present at the initial time of detection (therefore indicative of trapping of high nutrient source waters) they also show that the anomalies strengthen significantly in the later stages of the ACE lifetime in the South Indian Ocean, thereby supporting the eddy-Ekman mechanism resulting in enhanced productivity in ACEs. He *et al*. (2017) suggest that the eddy-Ekman effect is significant and triples the nutrient enrichment in the ML compared to solely the winter mixing effect. However, Dufois *et al.* (2014) propose the vertical flux of winter mixing to be on average approximately triple the size of the eddy-induced Ekman pumping vertical flux in the South Indian Ocean. Ultimately, a consensus on the relative importance of eddy-induced Ekman pumping and winter mixing in ACEs is still lacking.

Beyond the capability of eddies to induce enhanced biological productivity via the mechanisms discussed thus far, a process is discussed in the literature which may have indirect implications on eddy oxygen content concerns extreme ocean temperatures within eddies. Observations of eddies in the Tasman Sea region by Elzahaby and Schaeffer (2019) point to the role of warm-core ACEs as vehicles for enhancing marine heatwaves (MHWs) and stretching their influence to greater depths. The study finds that the depth of MHWs is strongly correlated to SSH anomalies (indicative of eddy presence), and notes that their findings are consistent with Rykova and Oke (2015) who similarly investigate SSH intensity, temperature anomaly and eddy-influence depth. The Elzahaby and Schaeffer (2019) findings have potential implications on ocean oxygen as higher temperatures are a constituent factor in driving decreased dissolved oxygen in the ocean via decreased oxygen solubility and increased upper ocean stratification effects (Keeling *et al.*, 2010). Furthermore, Elzahaby and Schaeffer (2019) find that a large majority (84%) of MHWs studied in the Tasman Sea occur within the boundaries of eddies. This suggests that the influence of eddy-enhanced MHW depth expansion is widespread in the eddy rich Tasman Sea region. To my best knowledge, there exist no studies investigating the role of eddy-enhanced MHWs on oxygen. However, I anticipate that, owing to the solubility and stratification effects of increased temperatures, warm-core ACEs may present an additional mechanism

for depleting oxygen across an extended depth range at the global mesoscale, especially so if the findings of Elzahaby and Schaeffer (2019) are applicable to other eddy rich oceanic regions.

2.3.2 – *Regional variation in eddy physical-biogeochemical mechanisms*

The regional variation in the relationship between SSH anomaly (indicative of eddy presence) and CHL anomaly (indicative of productivity) provides an insight into which mechanisms dominate which ocean regions. Gaube *et al*. (2014) use satellite measurements to produce a global map of the correlation between SSH anomaly and CHL anomaly [see Figure 1a in Gaube *et al*. (2014)]. In areas of positive SSH correlation, positive anomalies of CHL are believed to occur in ACEs, whereas it is it is implied that positive anomalies of CHL occur in CEs in areas of negative correlation. There is coherent regional structure in the positive/negative correlations (Gaube *et al.*, 2014; McGillicuddy, 2016). As such, this may form a suitable approximation of the distribution of regions which are dominated, for example, by either i) eddy trapping/eddy pumping mechanisms associated with CEs (the negative correlation regions) and ii) eddy trapping/winter mixing/eddy-induced Ekman pumping mechanisms associated with ACEs (the positive correlation regions). By this measure, EBUS are characterised by negative correlation, thereby suggesting that these regions will be dominated by eddy trapping/eddy pumping in CEs. Conversely, subtropical gyres, for example, appear dominated by positive correlation, thereby consistent with the findings of studies investigating enhanced CHL in ACEs in these regions (see section 2.3.1).

2.4 – *Eddy tracking strategies*

2.4.1 – *Modelling eddies*

Beyond eddy observational studies, global climate models with biogeochemistry represent a useful way of exploring eddies and biogeochemistry with a 'complete three-dimensional dataset' (i.e. longitude × latitude × depth) at global spatiotemporal scale. Biogeochemical float-style observational investigations are limited to snapshot views, whilst satellite altimetry based observational studies are prone to suffering distortion of data via the smoothing and interpolation methods that are needed to the convert raw satellite imagery to a gridded product (Chelton *et al.*, 2011b; Moreton *et al.*, 2020), as well as being limited to a surface-view only. Frenger *et al.* (2018) is one study that employs models to explore eddy biogeochemistry. However, generally, studies using modelling methods are rare, owing to the computational costs, which compromise the ability to run models at sufficient resolution to represent the mesoscale, plus the added expense of including biogeochemistry in the simulations (e.g. Hewitt *et al.*, 2020). As discussed in Section 2.1, the current generation of CMIP5 Earth System Models are lacking in skill with regards to ocean deoxygenation trends, potentially in part due to being run at insufficient resolution to resolve to the mesoscale. A model's ability to

resolve the mesoscale at different latitudes is governed largely by the ratio between the horizontal grid spacing of the model and the latitude-dependent Rossby radius of deformation – whereby the horizontal grid spacing must be significantly smaller than the Rossby radius in order for mesoscale features to be resolved (Hallberg, 2013; Moreton *et al.*, 2020). Therefore, there is motivation to strive towards higher resolution simulations, given the associated tangible benefits of resolving mesoscale eddies (i.e. Hewitt *et al.*, 2017).

It is generally acknowledged in the literature that models should be approaching eddy-permitting (1/4° horizontal spacing) and eddy-resolving (1/12°) resolutions, in order to begin properly resolving the mesoscale (e.g. Moreton *et al.*, 2020). Advances in computational power and efficiency have recently allowed for higher resolution Earth System Models, for example those in the next-generation CMIP6, to be run at these resolutions and are therefore able to resolve smaller scale physical features (Hewitt *et al.*, 2020). SSH fields from simulations of eddy-permitting resolution are considered to be sufficient to at least resolve instability-driven eddy-like disturbances and capture eddies at low to mid latitudes (Jansen and Held, 2014; Moreton *et al.*, 2020). Though improved relative to coarser resolution models, it is found that simulations at eddy-permitting resolution still lack the skill to fully resolve eddy features relative to both eddy-resolving simulations and observations. A study by Moreton *et al.* (2020), using HadGEM3-GC3.1 coupled climate model simulations (run at both eddy-permitting and eddy-resolving simulations) and an altimeter observational record, finds that eddy-permitting and eddy-resolving simulations produce only ≈ 40% and 63% of altimetry observed eddies respectively. A key reason for this is believed to be a severe underestimation of eddy genesis in EBUS regions and ocean interior gyres. This is likely due to poor representation of ocean currents in these regions. For example, topography, which provides frontal shear for eddy generation, may not be adequately resolved in the simulations (Deremble *et al.*, 2016; Moreton *et al.*, 2020). As discussed in Section 2.1, eddies in these regions play an important role in the transport of biogeochemically distinct waters into the ocean interior, and these are therefore effects which may be underestimated to a significant degree. So, whilst there have been improvements to resolving the mesoscale in higher resolution simulations – for example across CMIP generations approaching CMIP6 (e.g. Séférian *et al.*, 2020) – it is evident that there is still progress to be made in order to better constrain simulations of climate (Hewitt *et al.*, 2020).

2.4.2 – *Eddy identification and autonomous tracking*

Ocean surface-visible eddies leave an imprint on SSH (see Section 2.2) and as such 2-dimensional SSH fields are often used in order to identify and track eddies. The advent of satellite altimetry allowed first access to global high-resolution SSH fields for eddy tracking, and such products have been used in many studies to produce global observational datasets of eddies (e.g. Chelton *et al.*, 2007, 2011a) as well as to track eddies to analyse their influence on regional variations in ocean biogeochemistry at the ocean surface (e.g. Gaube *et al.*, 2013, 2014). In order to be able to isolate eddies for analysis, the autonomous identification and

tracking of these features in gridded observed satellite altimetry products (and/or in physical ocean model SSH fields) has become a vital tool. These methods allow for investigation of hundreds-of-thousands-plus features from one set of SSH data – something that is not possible in snapshot observational studies of individual eddies – therefore giving a more 'complete' census of eddies in the global ocean.

Chelton *et al.*, in their 2011b paper, document a brief history of autonomous eddy tracking methods development. The first attempt of such autonomous methods on satellite altimetry data was conducted by Isern-Fontanet *et al.*, (2003) who use the Okubo-Weiss (OW) parameter to identify areas where vorticity dominates strain (i.e. rotation exceeds deformation) and as such are thought to represent eddying cells. Later, additional eddy studies (e.g. Morrow *et al.*, 2004; Penven *et al.*, 2005; Chelton *et al.*, 2007) use OW-style analyses to track eddies in gridded satellite altimetry data and model simulations alike, though it also became apparent that there are problems with this method. Chelton *et al.* (2011b) discuss these issues as follows. Firstly, the OW method relies on specifying an OW parameter threshold value to identify an eddy, but a universal value is not optimal for the entire global ocean. Secondly, a velocity component is required to calculate the OW parameter, but this must be derived from noisy SSH fields. Lastly, the interiors of eddies identified through the OW method often do not correspond with closed contours of SSH such that it is possible for multiple vortices (occasionally of opposing polarity) to be contained within one OW-defined eddying region. With these issues in mind, Chelton *et al.* (2011b) deem the OW parameter to be an inadequate metric for eddy identification and instead favour identification directly from SSH fields, which removes the need for differentiation and thus avoids noisy SSH data issues.

Studies originally employing SSH-based identification methods, such as Fang and Morrow (2003) and Chaigneau and Pizarro (2005), still had the issue of having to define thresholds for identification, with globally applicable thresholds still difficult to determine. As such, studies have since sought to develop 'threshold-free' methods. For example, Chaigneau *et al.* (2008) employ a 'winding angle method', using derivatives of the SSH field, to identify closed contours of streamlines. However, this still involves derivation of SSH fields, as such once more opening the door to noisy SSH field related issues (Chelton *et al.*, 2011b). In an attempt to eliminate all issues discussed so far, Chelton *et al.* (2011b) devise a new method of SSH-based eddy identification. Here, the authors describe their method as 'threshold-free' whilst also avoiding the need for differentiating the already-noisy SSH field under the assumption that streamlines around eddies approximately follow closed contours of SSH anomaly. In this methodology, as described by Chelton *et al.* (2011b), SSH fields are firstly spatially filtered at each time-step to isolate mesoscale features and obtain maps of SSH anomaly. The method is made threshold-free by dividing an array of SSH values (from -100 to +100 cm) into 1cm increments. For ACEs (concave down SSH), the method iterates through each increment, starting from -100 cm and ascending until reaching a closed contour of SSH which satisfies a set of remaining identification criteria. This process is repeated for CEs (concave up SSH) but starting from +100 cm and

descending. Further details on additional criteria are available in Appendix B.2 of Chelton *et al.* (2011b) and in Section 3.2.1 of this thesis. Through this method, the perimeter cells of the located region approximate to the outermost SSH closed contour of the eddy feature. Chelton *et al.* (2011b) highlight a potential issue with this method as being that it is possible for the algorithm to identify regions with multiple extrema of SSH anomaly if eddies are close in proximity and contained within the same outermost closed contour of SSH. Mason *et al.* (2014) and Faghmous *et al.* (2015) represent attempts to improve upon some of the limitations in the Chelton *et al.* (2011b) SSH-based method by applying similar identification routines, but with differences in criteria, such as including local minima/maxima thresholds and introducing finer thresholding increments in Mason *et al.* (2014) and Faghmous *et al.* (2015) respectively.

Despite the acknowledged limitations in the Chelton *et al.* (2011b) method, it has proved a widely used method for eddy analysis work in this field of research. For example, Gaube *et al.* implement the methodology in various studies (2013, 2014, 2015), whilst Oliver *et al.* (2015) use it in order to explore the projected future changes biogeochemical characteristics of eddies in the Tasman Sea. Subsequently, a new version of the tracking routine has been created and named the "growing method" (Chelton and Schlax, 2016). Here, identified eddies are "grown" from individual SSH anomaly extrema by assessing whether neighbouring cells exceed an incremental range of thresholds. This method has the advantage of being more computationally efficient than other algorithms and is exemplified by Gaube *et al*. (2019) who use the method to explore eddy MLD globally. Finally, it is also worth noting that there exist additional novel eddy tracking methods outside of those primarily discussed in this review. These include, for example, a hybrid geometric-OW method (e.g. Halo *et al.*, 2014) as well as machine learning/neural network style strategies (e.g. Ashkezari *et al.*, 2016). The search for a leading eddy identification and tracking algorithm is thus still an ongoing competition, with each existing method having different advantages and disadvantages.

2.5 – *Eddies in future climate*

At present, there exists a paucity of literature on the subject of eddy future climate response. However, with eddies being established in the literature as potential redistributors of biogeochemically anomalous conditions, any potential changes to their prevalence and/or strength in future climates may be vital considerations when assessing future climate impacts, such as ocean deoxygenation. As such, I frame the following passage as a short note on potential considerations of eddies in future climates.

From a global perspective, Martínez-Moreno *et al.* (2021) analyse historical satellite altimetry records (across the period 1993–2020) and show significant increases in eddy activity in existing eddy-rich regions, such as the Southern Ocean, of 2–5% per decade, though with a decrease in tropical ocean activity. With these historical increases in mind, and given the reliance of eddy formation on instabilities in ocean currents, it

stands to reason, therefore, that the trend may be exacerbated around eddy-rich regions in more energetic future climates. For example, Oliver *et al.* (2015) make such a prediction for the Tasman Sea region and the increases in instabilities around the Eastern Australian Current separation point. Here, they predict that eddy kinetic energy is set to increase in the region in response to changes in wind stress curl over the ocean, whilst the proportions of ACEs:CEs may also shift in favour of ACEs in the region. Similarly, Matear *et al.* (2013) use an ocean eddy-resolving model to show increased eddy activity in the same Eastern Australia Current separation point under future climate. The study also states that this eddy activity increase will spark increases in nutrient supply to the upper ocean and therefore enhance productivity (and likely subsequent consumption of oxygen) in the oligotrophic waters of the Tasman Sea. The study also shows that this effect is not found in a similar simulation using a coarse resolution global climate model, implying that these models are inadequate for projecting future changes to eddy-induced ocean biogeochemistry. Again, studies investigating future changes to eddy activity are limited in number. However, if these projections (such as in Oliver *et al*., 2015) and Matear *et al.*, 2013) are applicable to other ocean regions with high-energy ocean currents – and as is suggested to already be happening in eddy-rich regions over recent decades (Martínez-Moreno *et al.*, 2021) – it is postulated that there will be future implications for eddy activity, intensities and ACE:CE proportions, and therefore biogeochemical responses, in other ocean domains.

Finally, the likely expansion of OMZ regions over the last ≈ 60 years is shown in observations (Stramma *et al.*, 2012a; Rhein *et al.*, 2013). However, future trends in OMZ expansion are less certain. Models do agree in general on a trend of future deoxygenation in the global ocean, however this is uncertain in subsurface tropical regions. Subsequently, the future of the lowest of oxygen concentrations in these regions, and therefore the OMZs, is unclear (Bopp *et al.*, 2013, 2017). If it is the case, however, that there is future expansion of the OMZs in tropical regions, this may result in a greater area of low oxygen water for eddies to trap, modify and transport west, which may add to eddies' ability to make significant contributions to the redistribution of oxygen in the global ocean.

3 – Data and Methods

This investigation uses an eddy-permitting ocean model and novel eddy tracking and analysis software suites to study eddy dynamical and biogeochemical properties and their role in oxygen variability in and around four EBUS regions.

3.1 – *Eddy-permitting ocean model simulations*

To complement valuable observational studies of eddies existing in the literature, numerical models provide fully spatiotemporally resolved fields to study eddy dynamics and associated biogeochemical properties.

Physical variables in this investigation (e.g. SSH) are provided by a data assimilation-free ocean reanalysis forced hindcast simulation produced at Mercator Ocean, FREEGLORYS2 version 4 (henceforth "FREEGLORYS2V4"). This simulation period spans January 1992 – December 2018 and is run globally at eddy-permitting spatial resolution (ORCA025 grid, 1/4° horizontal spacing), 75 vertical levels (≈ 1 m resolution in near-surface waters and ≈ 200 m in the deep ocean), and daily output frequency with the NEMO 3.1 ocean model (Madec, 2008). The model is forced at the surface by the ERA-interim atmospheric reanalysis from the European Centre for Medium-Range Weather Forecasts (ECMWF) (Perruche *et al.*, 2019). The oxygen field for this investigation is sourced from an assimilation-free biogeochemical hindcast simulation produced at Mercator Ocean, FREEBIORYS2 version 4 (henceforth "FREEBIORYS2V4", which uses the PISCES-v2 biogeochemical model (Aumont *et al.*, 2015) and is dynamically-forced by FREEGLORYS2V4. The simulation spans the same temporal period as FREEGLORYS2V4 and has an identical spatial grid (ORCA025, 75 vertical levels). The ERA-interim atmospheric reanalysis forces the ocean surface and the model biogeochemistry is initialised from World Ocean Atlas 2013 observations (Perruche *et al.*, 2019).

Due to data availability and storage constraints, the depth subset of the modelled data is limited to the range 0-300 m below the surface. However, it is anticipated that this interval is adequate for examining the depth imprint of the surface-visible eddies of concern in this investigation, given that this matches the depth range over which observations in the literature indicate oxygen to be substantially influenced by surface-intensifying eddies (e.g. Schütte *et al.*, 2016b).

3.2 – *Data analysis framework*

3.2.1 – *Eddy-oxygen census*

An eddy-oxygen census is produced over the full 1992–2018 model simulation period. To track the eddies in the physical FREEGLORYS2V4 simulation, a modified version of the SSH-based Oliver *et al.* (2015) implementation of the Chelton *et al*. (2011b) eddy tracking methodology is employed. Given that the data used in this investigation is of the same spatial and temporal resolution as that used in Chelton et al. (2011b), many of the cut-off values mentioned in subsequent discussion are identical. Broadly, an eddy is identified as such if it satisfies five criteria, devised by Chelton et al. (2011b) and implemented by Oliver et al. (2015). These are:

i) SSH is above or below a given critical SSH threshold value for ACEs and CEs, respectively.
ii) The number of grid cell pixels enclosed by each eddy lies between 8 and 1000 pixels.
iii) There is one or more local minimum or maximum SSH value for CEs and ACEs, respectively.
iv) The peak amplitude of the eddy exceeds 1cm.

v) The lateral extent of the eddy is less than 400km for latitudes poleward of 25°, and linear increase in this minimum cut-off up to the value of 1200km at the equator.

The detection of eddy features is performed on daily maps of SSH anomaly at time-step *i*. The tracks are then generated for each eddy across time by searching for each eddy centroid at time-steps *i* + 1, *i* + 2 … and so on, which lie within the distance of a given ellipsoid centred on the eddy at time-step *i* of length defined by the first baroclinic Rossby wave phase speed. (Chelton et al. 1998; 2011b). This ultimately produces tracks of eddies across space-time for the entirety of the analysis period (e.g. Figure 3.1). Further details on the algorithm can be found in Chelton et al. (2011b) Appendix B and Oliver *et al.* (2015) Appendix A.

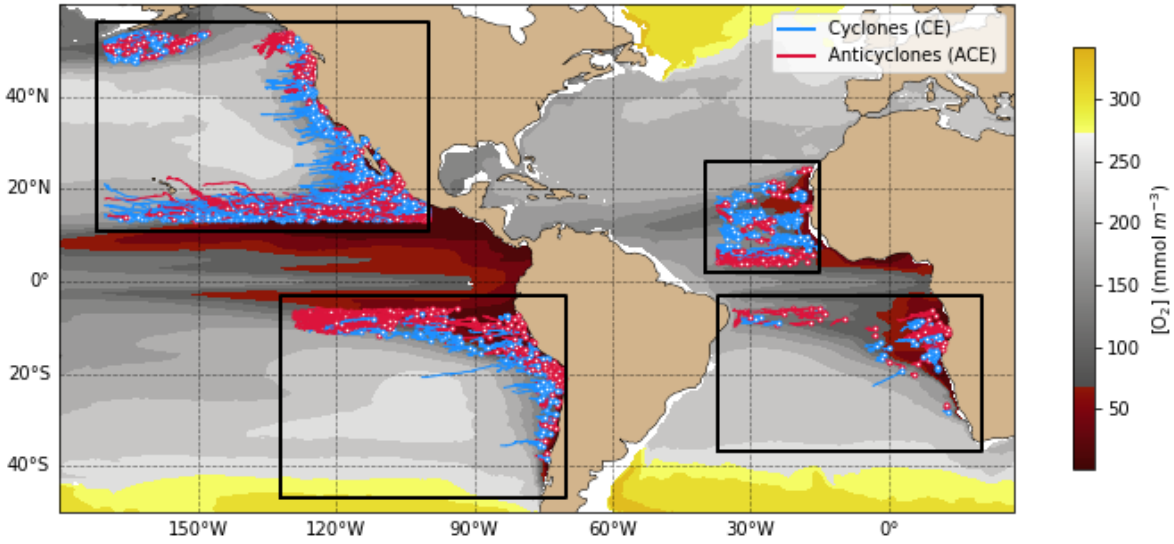

Figure 3.1 – Tracks of CEs (blue) and ACEs (red) in focus regions (marked by black boxes) across the period 1992-2018, which exceed a 4-week lifetime and originate in low oxygen waters (< 200 mmol m^{-3} depth averaged over ≈ 50–200 m). This constrained dataset does not match the datasets used in subsequent sections of this work and is shown only to illustrate the tracking procedure. Background shows climatological oxygen concentration at ≈ 200 m depth [mmol m^{-3}]. Initial detection points of eddies are indicated by white dots.

To isolate the oxygen signal associated with tracked eddies, the oxygen field beneath the eddy centroid from the surface to ≈ 300 m depth is extracted in the FREEBIORYS2V4 biogeochemical simulation. To explore the balance of physical and biogeochemical processes occurring within the eddies, the oxygen signal is decomposed into apparent oxygen utilisation (AOU) and oxygen saturation (O_2sat) components, where

$$AOU = O_2sat - [O_2], \quad [1]$$

and O_2sat is calculated according to the solubility constants as presented in Weiss (1970). Anomalies for key variables, including [O_2], AOU and O_2sat, are produced relative to the non-eddying background field. The non-eddying background is estimated by spatiotemporally filtering the model fields to remove the mesoscale;

using a rolling monthly temporal window and 15° longitude, 5° latitude spatial cut-off wavelengths, following (Schütte *et al.*, 2016a).

Tracking is performed in four focus regions to identify eddies in and around EBUS of the North-Eastern Atlantic (NEA), South-Eastern Atlantic (SEA), North-Eastern Pacific (NEP), and South-Eastern Pacific (SEP). Figure 3.2 demonstrates the spatial coverage and counts of CEs and ACEs in each focus region. A constraint of a minimum 1-week lifetime is applied to the eddy dataset, in order to avoid including the effects of spurious phenomena in the findings.

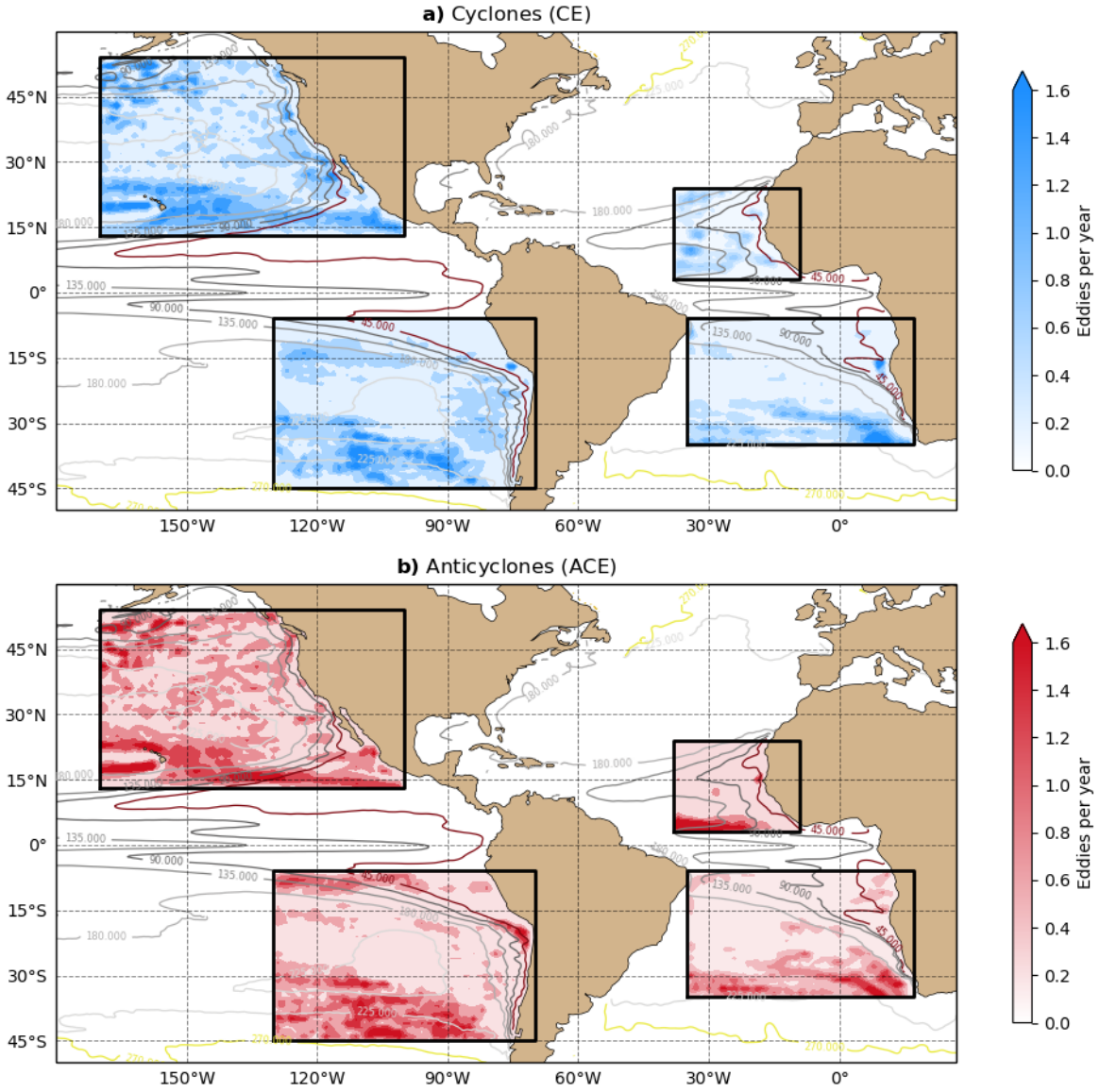

Figure 3.2 – (a) CE and (b) ACE counts per year in focus regions (marked by boxes), which exceed a 1-week lifetime, across the simulation period 1992–2018, in 1°x1° bins. Background contours show climatological oxygen concentration at ≈ 200 m depth [mmol m^{-3}].

3.2.2 - *Eddy property calculations*

For each tracked eddy centroid location (time, latitude, longitude); lifetime, radius, area and amplitude are calculated as part of the original Oliver et al. (2015)/Chelton et al. (2011b) method. In addition, dynamics metrics of rotational velocity (*U*), translational velocity (*c*) and nonlinearity (*U/c*) are calculated here in order to later test the impact of eddies of differing dynamical strength on biogeochemical consequences. These calculations are carried out as follows.

a) Eddy rotational velocity (*U*) [m s^{-1}] is calculated for each detected eddy feature by:

$$U = gf^{-1} * A/L \text{ (Chelton } et\ al.\text{, 2007, 2011b)} \quad [2]$$

Where *g* = gravitational acceleration constant [m s^{-2}], $f = 2\Omega sin\varphi$ (Coriolis parameter) [rad s^{-1}], *A* = eddy amplitude [m], and *L* = eddy radius [m].

b) Eddy translational velocity (*c*) [m s^{-1}] is calculated at time-step *i* based on the distance travelled between eddy centroids at time-steps *i* – 1 and *i* + 1 across this 48-hour period as (assuming Earth as a perfect sphere):

$$c = \frac{distance}{time} = \frac{Arccos(x) * R * \frac{\pi}{180}}{t} \text{ (Oliver } et\ al.\text{, 2015)} \quad [3]$$

$$\text{Where } x = \sin(lat_{i+1}) * \sin(lat_{i-1}) + \cos(lon_{i+1} - lon_{i-1}) * \cos(lat_{x+1}) * \cos(lat_{x-1}) \quad [4]$$

And *R* = Earth equatorial radius [m], *t* = 172,800 [seconds in 48 hours].

c) The nonlinearity (*U/c*) for each eddy type is subsequently calculated as a ratio of rotational velocity (*U*) to translational velocity (*c*) of the eddy, i.e.

$$nonlinearity\ (U/c) = \frac{rotational\ velocity\ (U)}{translational\ velocity\ (c)} \text{ (Chelton } et\ al.\text{, 2011b)} \quad [5]$$

3.2.3 – *Eddy low oxygen extreme events methodology*

To explore low oxygen extremes in eddies relative to non-eddying cells (Section 4.3), we assess the interaction between eddies/non-eddies and 'low oxygen extreme events'. Low oxygen extreme events are defined as instances where the depth-minimum oxygen concentration in a given location falls below the 1st

percentile value of the climatological depth-minimum oxygen concentration for that location across the full simulation period 1992-2018. This fixed percentiles-based approach is similar to the work of Frölicher *et al.* (2018) and their definition of extreme marine heatwave events – though with the use of above-99th percentile threshold for a heatwave in contrast to the below-1st percentile criterion used in this report for low oxygen extreme events.

In order to investigate the extreme events, three metrics to characterise the behaviours of CE-/ACE-events in different OMZ regions are also defined. The first two of these metrics are similar to those used by Oliver *et al.* (2019) in the context of marine heatwaves, but are here instead adapted to eddy-oxygen events:

i) Frequency – the number of CEs/ACEs/non-eddies which simultaneously experience low oxygen extreme events, expressed as a proportion relative to the total number of CEs/ACEs/non-eddies [%]
ii) Intensity – the average oxygen concentration within CE/ACE/non-eddy low oxygen extreme events, with the intensity of each event defined as the minimum across 0-300 m depth beneath the eddy centroid [mmol m^{-3}].

In addition, to quantify the spatial distribution of eddy low oxygen extreme event influence, iii) percentage contribution is defined as the number of CE/ACE low oxygen extreme event days expressed as a proportion relative to the total number of low oxygen extreme event days (CE/ACE/non-eddy types combined total), in each grid cell location [%].

With regard to low oxygen extreme event analysis in Section 4.3, only low oxygen extreme events identified outside of the natural OMZs are considered, where oxygen concentrations are permanently low and therefore skew the fixed percentiles-based methodology. Based on an OMZ criterion demonstrated by Karstensen *et al.* (2008) and described as "stringent", a threshold value of 45 mmol m^{-3} is used to identify the OMZ locations, where any location with a climatological oxygen value below this threshold at any depth level is masked. Thus, Section 4.3 focusses on the interaction between eddies and the extreme state of oxygen outside of the permanent OMZs.

3.3 – *Ocean model validation*

Validation of the FREEGLORYS2V4 eddy field is achieved by comparison against a gridded (1/4° horizontal spacing) SSH satellite observational product distributed by the Copernicus Marine Environment Monitoring Service (CMEMS) (previously AVISO+) (Pujol and Mertz, 2020). This comparison is carried out for the eddy fields tracked over the period 1993-2018, which is the longest overlapping period for both model and

observations. Tracking results show that many more eddies are resolved in the observations compared to the model, consistently across all focus EBUS regions (Table 3.1). FREEGLORYS2V4 simulates up to ≈ 40% of the number of eddies tracked in the observations (for eddies > 1-week lifetime in the NEP region). For those eddies which have lifetimes in exceedance of 4 weeks, the model produces ≈ 30% of eddies found in observations in the NEP region and ≈ 9% of the number of > 4-week observed eddies in the NEA region. It is shown, therefore, that the simulation is less skilful in the NEA region (for both shorter and longer lifetime eddies) whilst performing better in the NEP region, with the SEA and SEP regions falling in between the two extremes. These findings are broadly consistent with those of Moreton *et al.* (2020) who note that, as a global average, an eddy-permitting simulation of the HadGEM3-GC3.1 coupled climate model produces ≈ 40% of the number of eddies found in the observations. This same study states that there is particular underestimation in EBUS regions, therefore echoing the findings of the validation in this report where proportions are frequently below this global-average 40%. Eddy-resolving simulations (1/12° horizontal spacing) are considered preferable for resolving the mesoscale field (e.g. Moreton *et al.*, 2020), but the eddy-permitting model used in this investigation facilitates a compromise between the need for sufficient computational resource to run multiyear simulations with biogeochemistry at daily output frequency, whilst still representing the mesoscale.

Table 3.1 – Number of eddies (total CEs and ACEs) in FREEGLORYS2V4 (model) and observations (obs) for the common period of 1993-2018.

Region	Data	> 1 week	> 4 weeks
NEA	Model	1,910	331
	Obs	12,777	3,790
	Model % of Obs	**14.95**	**8.73**
SEA	Model	7,176	1,890
	Obs	28,090	8,776
	Model % of Obs	**25.55**	**21.54**
NEP	Model	24,813	6,560
	Obs	61,319	22,126
	Model % of Obs	**40.47**	**29.65**
SEP	Model	19,940	4,412
	Obs	59,310	21,120
	Model % of Obs	**33.62**	**20.89**

In terms of physical characteristics of the eddies tracked in the FREEGLORYS2V4, it is found that the model is able to adequately reproduce eddy lifetime and amplitude behaviours when compared to the satellite observational product (Figure 3.3). Lifetime distributions closely match between model and observations, whilst both model and observations show a peak amplitude of ≈ 1.5 cm. Considering the lateral extent of the

eddies tracked, however, there is a mismatch between the model and observations. The model shows a high bias in terms of radius and area relative to the observations. The distribution of eddy surface radius is skewed towards higher values in the model (model peak frequency at ≈88 vs. ≈ 55 km in observations), and this effect is naturally mirrored in the eddy area values. This is expected given that simulations at eddy-permitting resolution tend to resolve only the larger portion of the mesoscale (e.g. Hallberg, 2013; Moreton *et al.*, 2020).

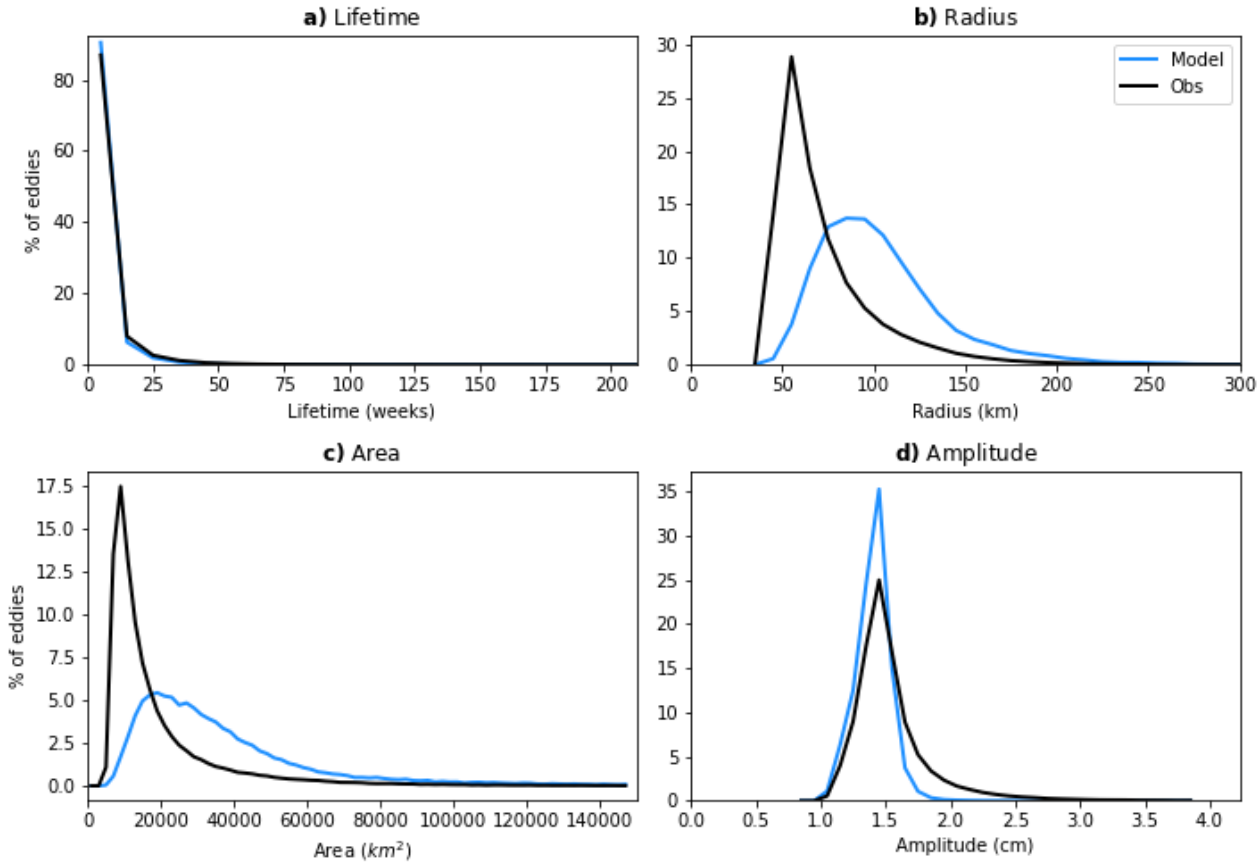

Figure 3.3 – Frequency distributions of eddy a) lifetime, b) radius, c) area, and d) amplitude in eddies tracked (those which exceed 1-week lifetimes, both CEs and ACEs) in model simulations (blue line; FREEGLORYS2V4) and observations (black line; CMEMS), across the period 1993-2018. All eddies tracked in the four focus regions of this study are composited to form a singular EBUS distribution for each variable.

In order to assess the skill of the hindcast biogeochemical ocean model simulation, a simple experiment is designed to compare the model oxygen output to World Ocean Atlas 2018 (WOA2018) oxygen field. WOA2018 is a gridded, objectively-analysed climatological mean field of ocean oxygen based on in situ measurements (Garcia *et al.*, 2019b). The highest horizontal resolution available for the record is 1°. As such, the model field is interpolated onto the same resolution grid to allow for direct comparison. A key limitation of this dataset is limited spatial data availability in some regions and at deeper levels. In addition, measurements are, for the most part, only available at irregular temporal intervals (Garcia *et al.*, 2019a). Finally, the data is only available as a mean field over the period 1955-2018, whilst the hindcast model

simulation spans only 1992-2018. As such, there may be an added climate signal across a longer time-span in the observations. The validation procedure shows that the model represents well the distribution of tropical OMZ waters (Figure 3.4a), with some inconsistencies, however, in the focus regions relative to the observations (Figure 3.4c). In the NEA and SEA, simulated oxygen values at ≈ 200 m depth are low relative to observations in coastal regions (up to +60 mmol m^{-3} difference in some areas), whilst they are generally higher in the open ocean areas. Of all EBUS regions, the NEP shows the most agreement across model and observations with differences generally within the range of ± ≈ 10 mmol m^{-3}. The SEP appears to show higher oxygen concentrations in the simulation, with the difference being up to ≈ -60 mmol m^{-3}. Model-observation offsets in the OMZs are a widely reported deficiency in current generation IPCC-class numerical models (e.g. Stramma *et al.*, 2012a; Cabré *et al.*, 2015). However, it has been shown that models on ORCA025 eddy-permitting grids, such as those employed in this report, are more skilful in simulating the OMZs (Berthet *et al.*, 2019).

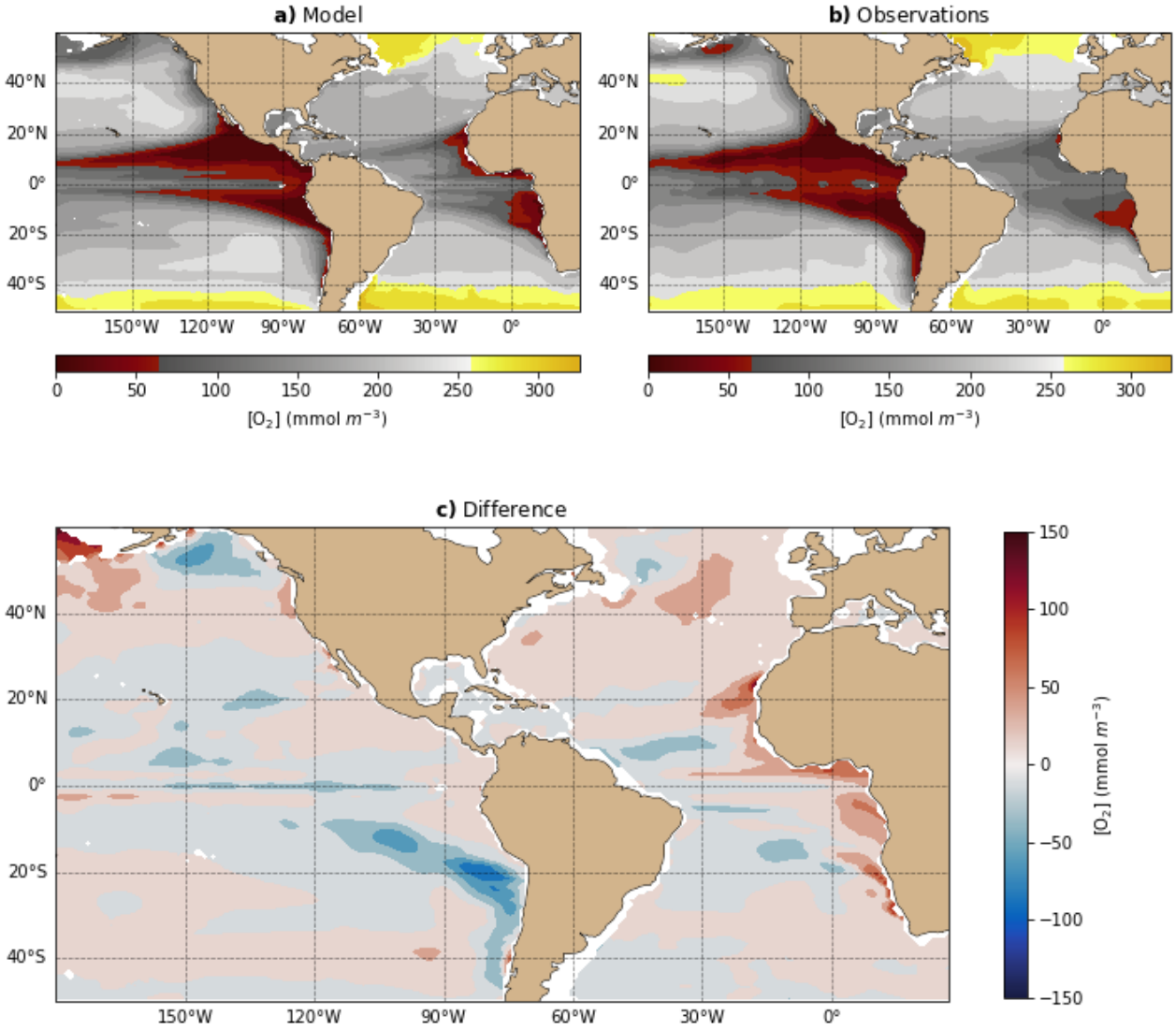

Figure 3.4 – a) FREEBIORYS2V4 modelled mean oxygen concentrations (across 1992-2018), b) WOA2018 observed mean oxygen concentrations (across 1955-2018), and c) difference between mean oxygen concentrations in WOA2018 and model simulation (observations – model), at ≈ 200 m depth.

4 – Results

Initially, to evaluate the profiles of westward propagating eddies crossing the oxygen gradient from EBUS waters to the more oxygenated open ocean, eddies analysed in Sections 4.1 and 4.2 are further constrained by those which originate in low oxygen waters, i.e. below 200 mmol m^{-3} depth averaged over ≈ 50–200 m; as in Frenger *et al.* (2018).

4.1 – *Eddy-oxygen profiles*

Frequency distributions of oxygen concentrations across the depth range ≈ 50–200 m beneath the centroid of eddies, demonstrate a propensity for CEs and ACEs to exhibit larger proportions of low oxygen values relative to regional climatologies (Figure 4.1). Specifically, eddies are often shown to contain hypoxic and even suboxic conditions. For example, in the SEA, there is a distinctly elevated proportion of CE grid cells associated with hypoxic waters compared to the climatological baseline, ≈ 44% of cells beneath the CE centroid across the depth range ≈ 50-200 m are associated with hypoxic or suboxic waters (i.e. < 60 mmol m^{-3}) versus ≈ 3% in the regional climatology. Meanwhile, ACEs in this same region also show elevated proportions of hypoxic/suboxic waters (≈ 26%) compared to the climatological baseline, but to a lesser extent when compared to CEs. The SEP region's CEs and ACEs show consistently high frequencies of both hypoxic and suboxic waters relative to the regional climatology. In the NEP, there is a relatively high proportion of both CEs and ACEs associated with suboxic waters, with ≈ 8% of grid cells falling below the 5 mmol m^{-3} suboxic threshold for both eddy types.

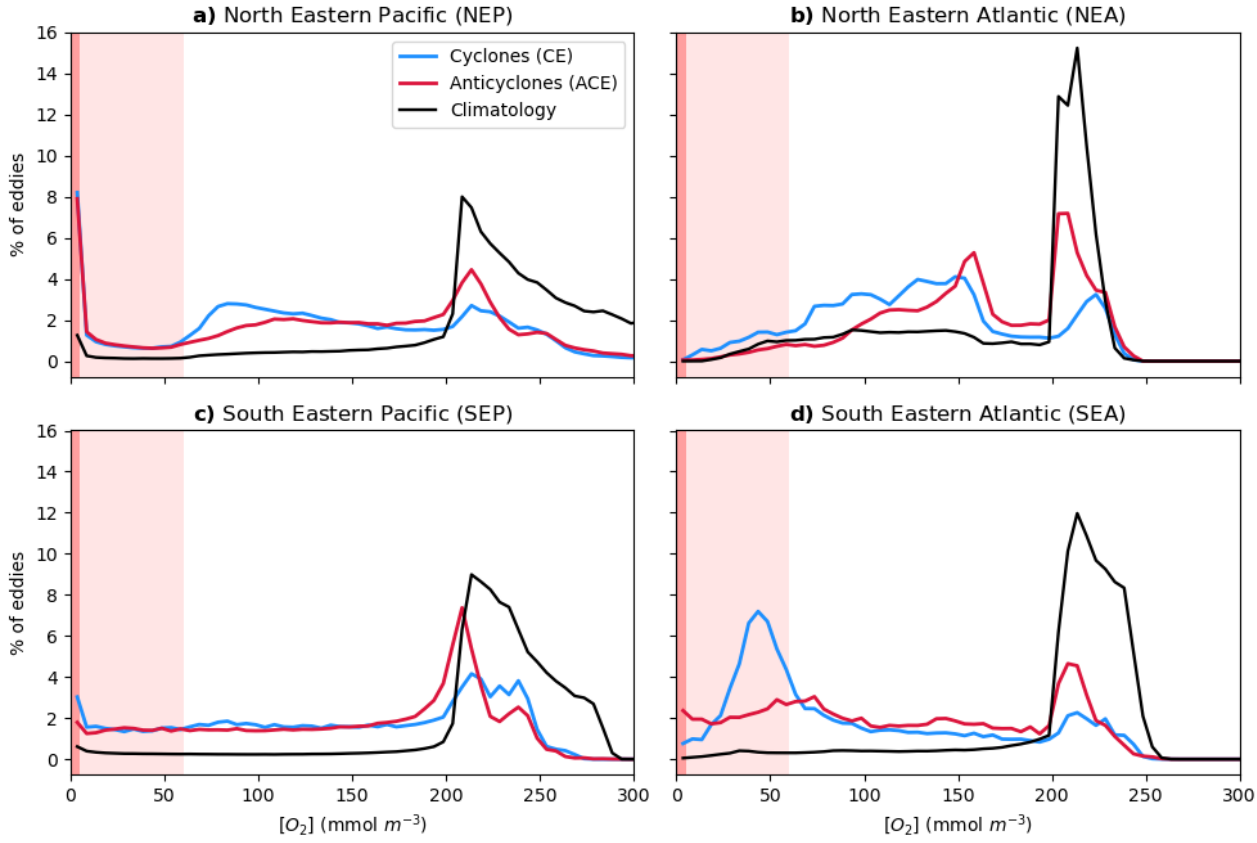

Figure 4.1 – Frequency distributions of dissolved oxygen concentration (5 mmol m^{-3} bins) beneath the centroids of CEs (red line), ACEs (blue line) and regional climatology (black line), at depth levels within the range ≈ 50-200 m, in focus regions. CEs and ACEs are tracked over the period 1992-2018 and are constrained by those which originate in low oxygen waters (< 200 mmol m^{-3}). Light red shading represents approximate hypoxic concentrations (< 60 mmol m^{-3}), darker red shading shows approximate suboxic concentrations (< 5 mmol m^{-3}).

The modulation of oxygen by eddies is evident in the oxygen anomaly profiles of both CEs and ACEs. The distributions of oxygen anomalies beneath the centroids of eddies, relative to a smoothed non-eddying background oxygen field, show a tendency for CEs to be more negatively anomalous than ACEs (Figure 4.2). Differences between CE and ACE distributions (grey bars in Figure 4.2) show a prevailing dominance of CEs in the increasingly negative oxygen anomaly bins in all regions.

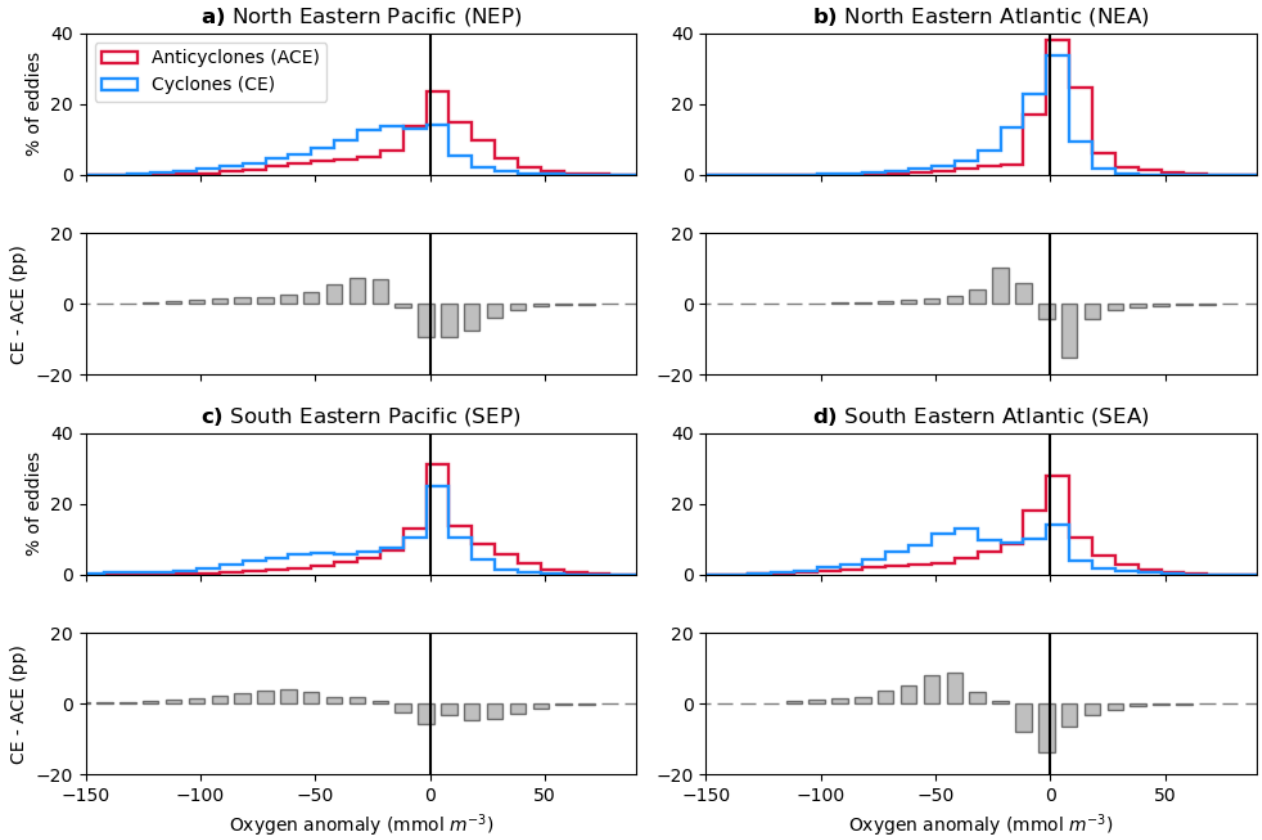

Figure 4.2 – Distributions of eddy oxygen anomaly (10 mmol m^{-3} bins) at depth levels within the range ≈ 50-200 m beneath the centroids of CEs (blue) and ACEs (red) which originate in low oxygen waters (< 200 mmol m^{-3}) in focus regions, tracked over the period 1992-2018. Grey bar subplots show difference between CE and ACE distributions (i.e. difference between red and blue lines) in terms of percentage point (pp) difference within each oxygen anomaly bin.

Composite oxygen anomaly profiles, as a function of depth, beneath eddy centroids further emphasise modulation of subsurface oxygen by eddies, with anomalies being most pronounced beneath the mixed layer at ≈ 50–200 m depth (Figure 4.3). CEs are shown to be more oxygen depleted – with statistically significant negative anomalies below ≈ 100 m depth – relative to the non-eddying background field across all regions apart from the NEA. SEA CEs exhibit the largest negative oxygen anomalies of up to ≈ -80 mmol m^{-3} at 80 m depth. Negative oxygen anomalies associated with ACEs in the NEP, SEP and SEA regions are consistently less intense than for CEs, and ACE responses are statistically indistinguishable from zero. Unlike other regions, the NEA shows overall positive mean oxygen anomaly in ACEs, though with considerable variability around the mean value.

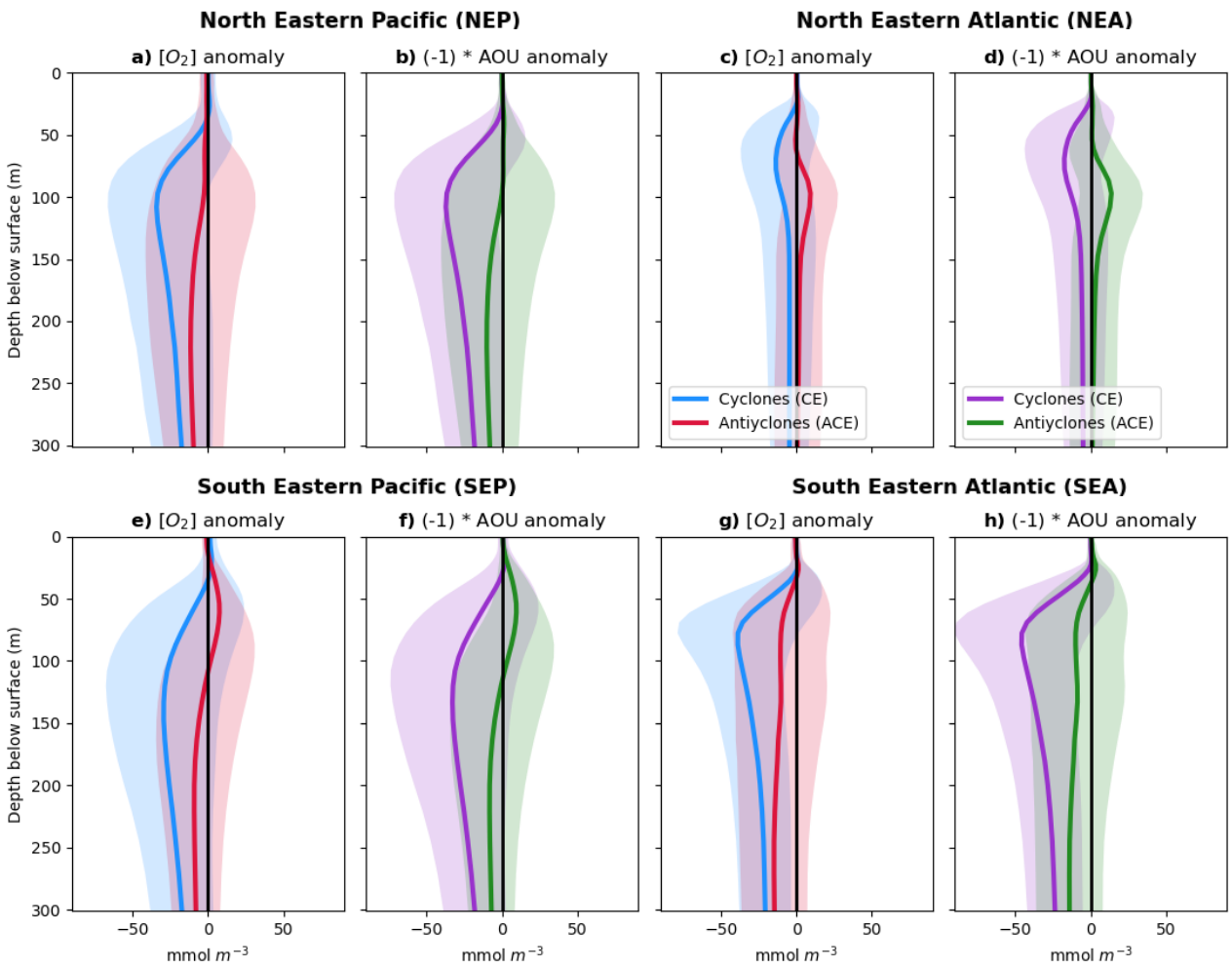

Figure 4.3– Composite oxygen (blue for CEs, red for ACEs) and (-1)*AOU (purple for CEs, green for ACEs; mmol m^{-3}) anomaly depth profiles beneath centroids of CEs and ACEs which originate in low oxygen waters (< 200 mmol m^{-3}) in focus regions, tracked over the period 1992–2018. Anomalies expressed relative to a non-eddying background field. Solid lines are mean values of all eddies at each model depth. Shading represents ± 1 standard deviations.

The eddy composite oxygen signal is decomposed into AOU (Figure 4.3) and O_2sat (Figure 4.4) components, and it is noted that negative oxygen anomalies of CEs are dominated by synchronous increases in AOU (Figure 4.3), indicating that the oxygen signal is predominantly due to enhanced consumption in the waters trapped by within the rotation of the eddies. Consistent with overall oxygen anomalies, ACEs show either less intense AOU anomalies and/or anomalies of varying sign over depth, and there is lower confidence in the dominant sign of change. It is also shown that the cold-cored CEs generally demonstrate positive anomalies of O_2sat, and therefore largely enhanced saturation of oxygen within their waters (Figure 4.4). Meanwhile, warm-core anticyclones tend to exhibit negative anomalies of O_2sat. The largest anomalies of AOU and O_2sat are shown in CEs in the SEA, where standard deviations demonstrate statistically significant anomalies. The enhanced oxygen utilisation in CEs via AOU is partially offset by the simultaneous increases in O_2sat due to the increased solubility of oxygen in the cold-core CEs. For example, in the SEA, CEs exhibit a mean AOU anomaly of ≈ -45

mmol m^{-3} at ≈ 100 m depth. This is counteracted – albeit to a limited extent – by ≈ 7 mmol m^{-3} mean O_2sat anomaly at the same depth (net oxygen anomaly ≈ -38 mmol m^{-3}).

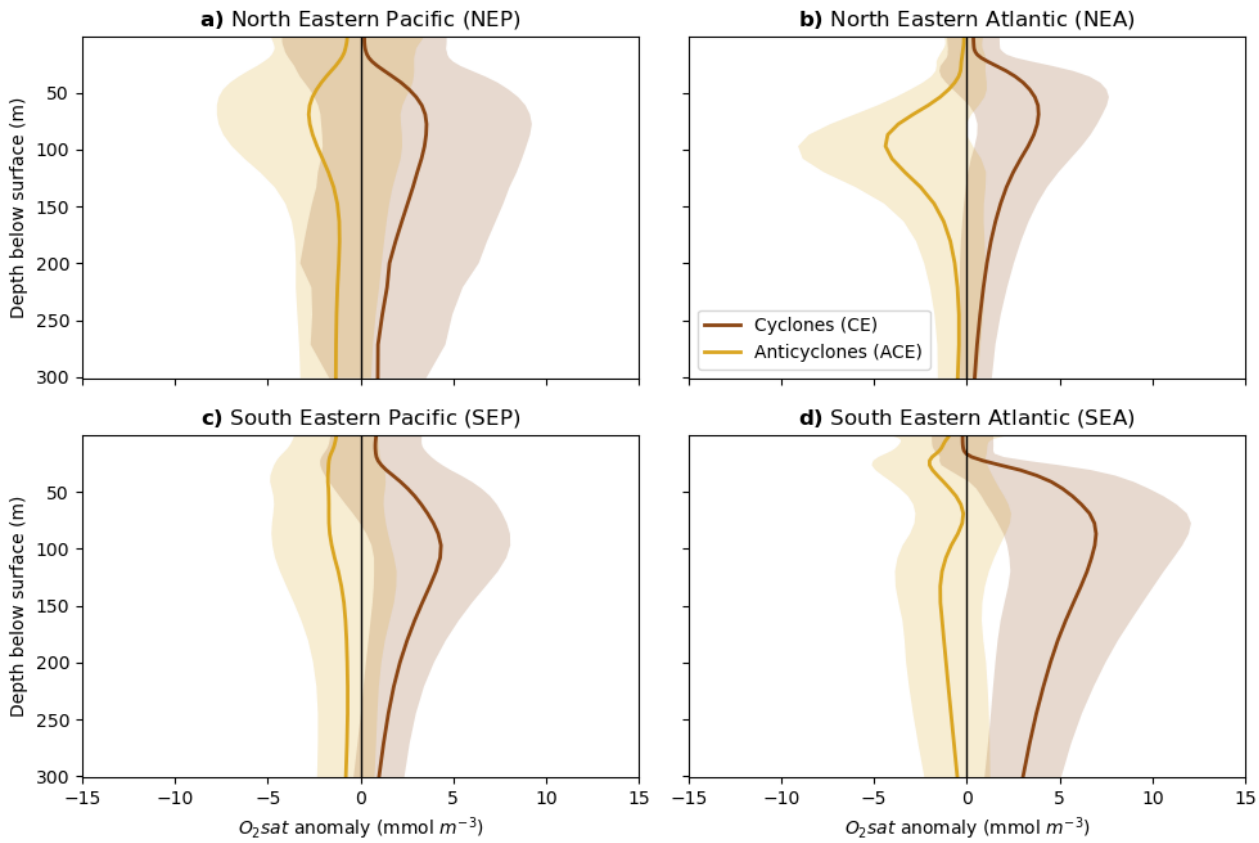

Figure 4.4 – Composite O_2sat anomaly depth profiles beneath the centroids of CEs (brown) and ACEs (yellow) which originate in low oxygen waters (< 200 mmol m^{-3}) in focus regions, tracked over the period 1992-2018. Anomalies expressed relative to a non-eddying background field. Solid lines are mean values of all eddies at each model depth, thereby forming a composite depth profile. Shading represents ± 1 standard deviations.

4.2 – *Characterisation of low oxygen eddies*

By means of further exploration into the oxygen response in eddies, the defining physical characteristics of a strongly deoxygenating eddy – propagating westward along an oxygen gradient from low oxygen origin waters to the more oxygenated open ocean – are examined.

Firstly, the relationship between eddy surface radius and oxygen anomaly is assessed. It is shown that eddy surface radius explains a moderate amount of the variability in oxygen anomaly in eddies in all regions, whereby anomalies are increasingly negative at smaller radii (Figure 4.5). Generally, the positive relationships between radius and oxygen anomaly are stronger for CEs compared to ACEs in all regions. The relationships are shown to be strongest in the case of CEs in the SEP and SEA regions (r = 0.60 and 0.58 respectively). The

NEA region demonstrates the weakest relationship of all regions with regard to both CEs and ACEs. In all instances, the relationships are shown to be statistically significant ($p < 0.01$).

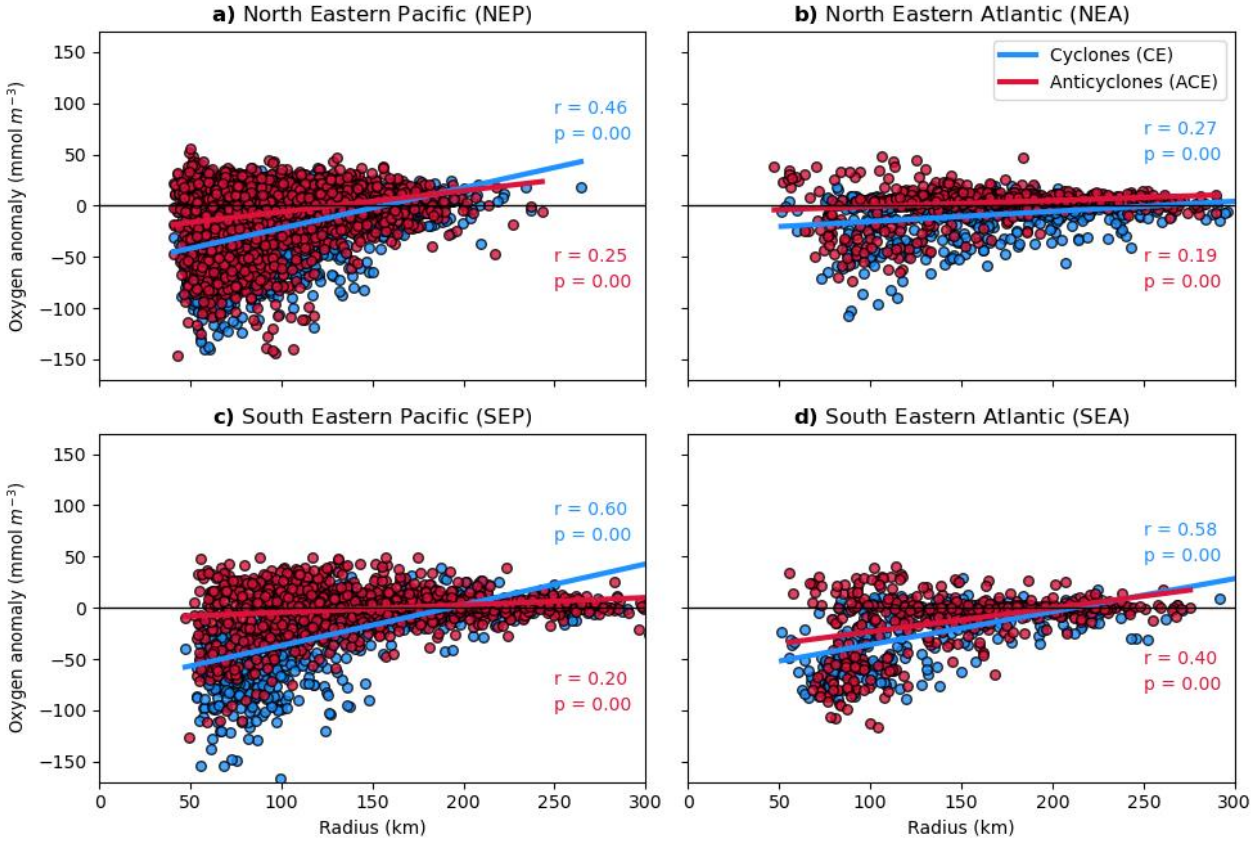

Figure 4.5 – Surface radius vs. oxygen anomaly of CEs (blue) and ACEs (red) which originate in low oxygen waters (< 200 mmol m^{-3}) in each EBUS focus region, tracked over the period 1992-2018. For each eddy, oxygen anomaly values are depth averaged over ≈ 50-200 m, and temporally averaged across the eddy lifetime. Surface radius values are averaged across eddy lifetime. Solid lines show ordinary least squares regression, and text shows accompanying regression statistics.

Beyond the eddy radius, the amplitude, rotational velocity and nonlinearity of eddies – and the associated oxygen anomaly response – are investigated (Figure 4.6). When all data from the focus regions are combined, there is a statistically significant, yet very weak negative relationship evident between both CE and ACE amplitude and oxygen anomalies, whereby larger amplitude eddies are weakly associated with increasingly negative oxygen anomalies (r = -0.10 and -0.09 for CEs and ACEs respectively; Figure 4.6a). In addition, there appears no meaningful relationship between eddy rotational velocity and oxygen anomaly, and it is shown to be statistically insignificant (Figure 4.6b). Meanwhile, there is a statistically significant, but weak negative relationship between CE nonlinearity and oxygen anomaly, potentially implying that more nonlinear eddies may be to some extent associated with more negative oxygen anomalies (r = -0.20, Figure 4.6c).

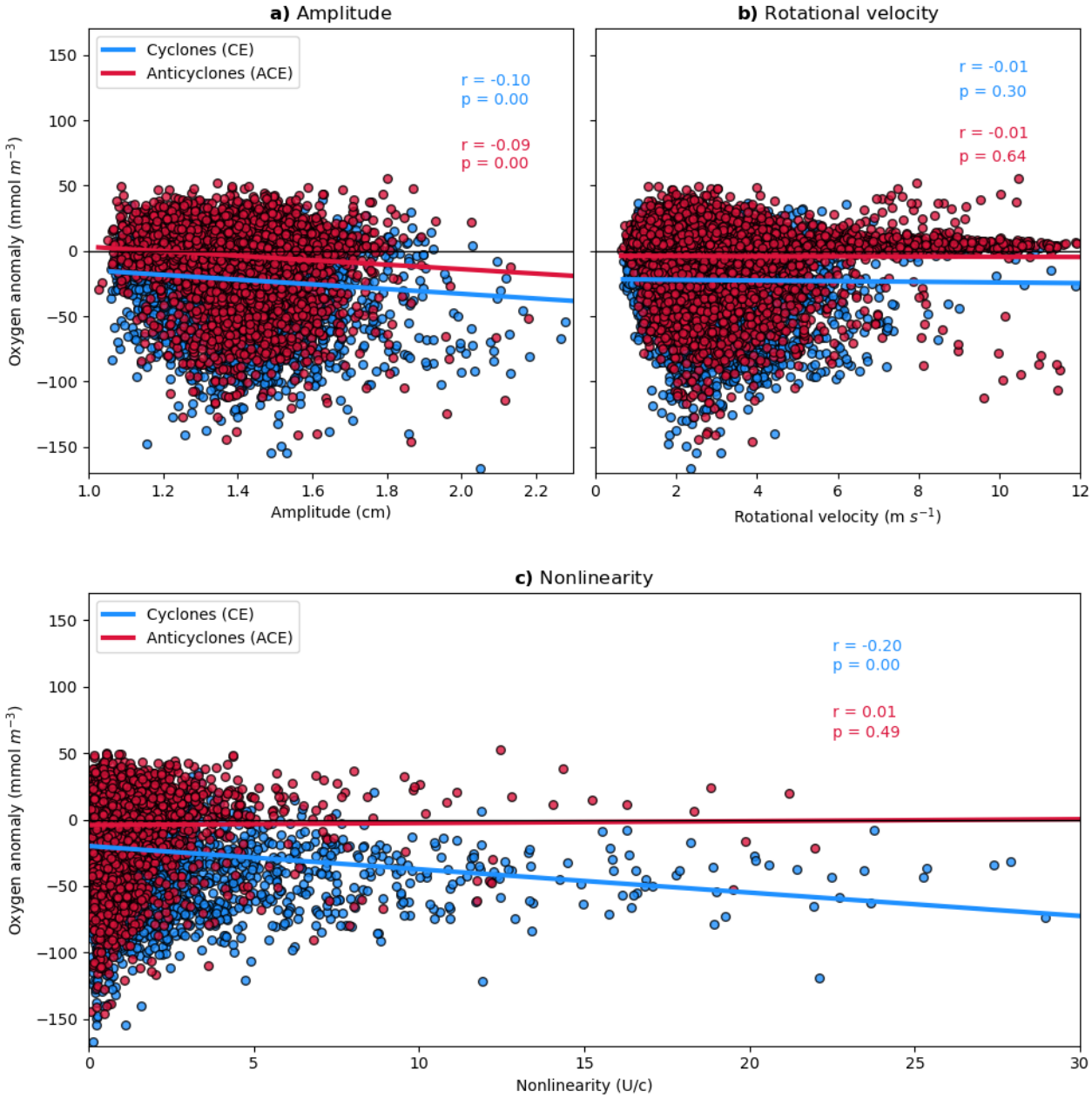

Figure 4.6 – (a) Eddy amplitude, (b) rotational velocity and (c) nonlinearity vs. oxygen anomaly in CEs (blue) and ACEs (red) which originate in low oxygen waters (< 200 mmol m^{-3}), tracked over the period 1992-2018. CE and ACE data from each focus region is combined to produce a global EBUS dataset for each variable. For each eddy, oxygen anomaly values are depth averaged over ≈ 50-200 m, and temporally averaged over the eddy lifetime. Amplitude, rotational velocity and nonlinearity values are averaged over the eddy lifetime. Solid lines show ordinary least squares regression, and accompanying text shows regression statistics.

4.3 – *Eddy low oxygen extreme events*

Considering the potential importance of eddies in driving extremely low oxygen extreme events in and around EBUS regions (e.g. Frenger et al., 2018), the low oxygen extremes for CEs and ACEs are characterised here in the study's focus regions. An extreme event day is defined where depth-minimum

oxygen concentrations fall below the 1st percentile of climatological depth-minimum oxygen (see Section 3.2.3). As stated in Section 3.2.3, for this, only eddies outside of the permanent OMZs are considered.

Figure 4.7 shows the frequency and intensity of low oxygen extreme events (see Section 3.2.3) associated with CEs and ACEs in each focus region. Generally, it is shown that the frequency of low oxygen extreme events is higher in eddies compared to low oxygen extreme events identified in non-eddying locations (Figure 4.7a). For example, in the NEP and NEA, the frequency of CE low oxygen extreme events is between ≈ 5-6% of total CEs in both regions, compared to < 1% in non-eddying locations. In the SEP and SEA, ACE low oxygen extreme frequency exceeds that of CE events (≈ 4-7% of ACEs, ≈ 2% of CEs, < 1% of non-eddy locations). Furthermore, there is some tendency for CE low oxygen extreme events to exhibit higher intensity (i.e. lower depth-minimum oxygen concentrations) beneath eddy centroids relative to both ACE and non-eddying events, though with some substantial variability around mean values (Figure 4.7b). Relatively more intensely low oxygen extreme events are most evident in CEs tracked across the SEP region, where the average depth-minimum is ≈ 105 mmol m^{-3} for CE low oxygen extreme events, compared to ≈ 207 and ≈ 140 mmol m^{-3} in ACE and non-eddying events, respectively.

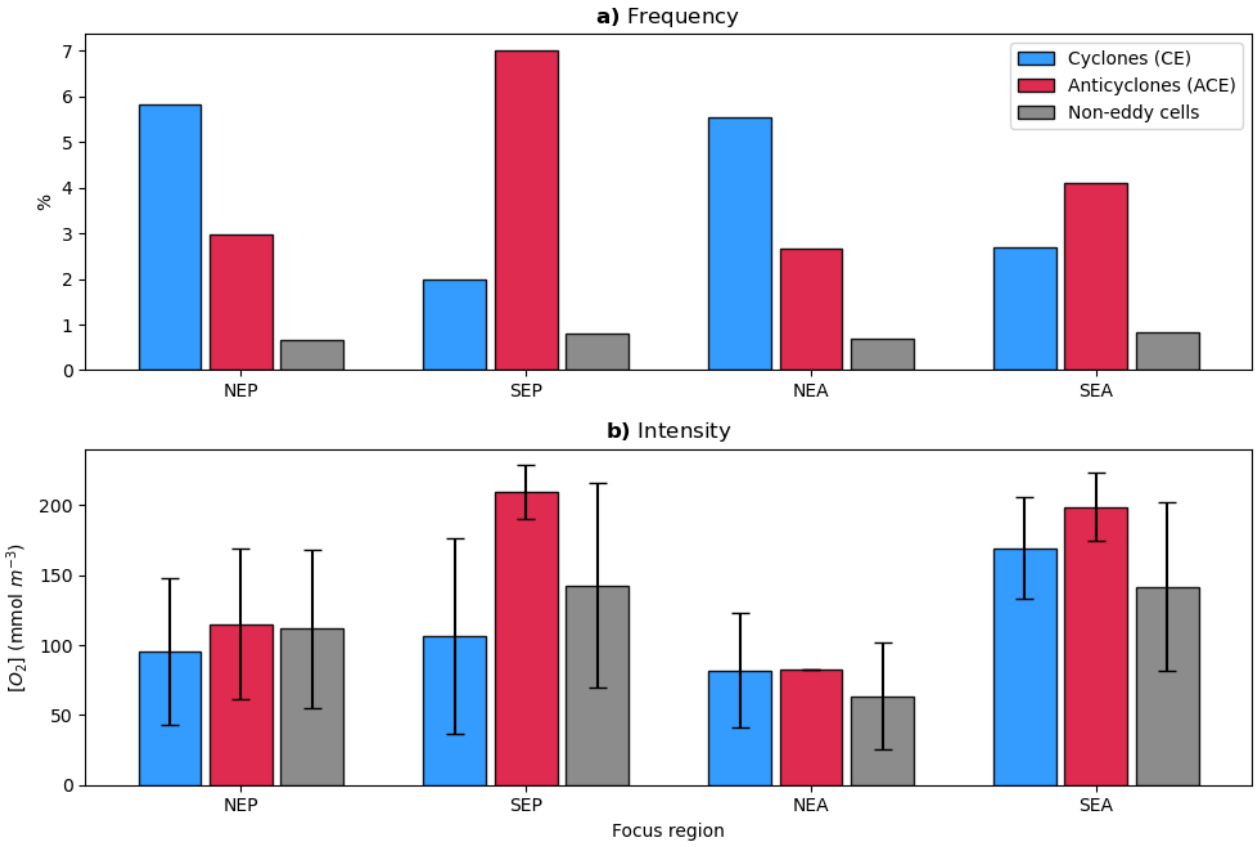

Figure 4.7 – (a) Frequency (percentage of total CEs/ACEs/non-eddies which experience low oxygen extreme events) and (b) mean intensity (minimum oxygen concentration within CE/ACE/non-eddy low oxygen extreme events across 0-300 m depth beneath the eddy centroid) of CE (blue bars), ACE (red bars) and non-eddy (grey bars) oxygen extreme events

in focus regions, across the period 1992-2018. Error bars show ± 1 standard deviation. Eddies in permanent OMZs are not shown.

Finally, the spatial contribution of eddies to the total number of low oxygen extreme events is presented. Figure 4.8 shows the percentage contribution of CEs and ACEs to the total number of < 1st percentile low oxygen extreme event days across 1°x1° bins in each focus region. The Pacific regions show substantial contributions of eddies to overall low oxygen extremes, with both CEs and ACEs associated with up to ≈ 15% of all low oxygen extreme event days across large areas of the NEP and SEP regions. CEs and ACEs both exhibit regionally distinct contributions to low oxygen extreme event days. In the Pacific regions, for instance, CEs contribute more substantially to low oxygen extremes in eastern boundary regions and ACEs more in the western parts. Meanwhile, the percentage contributions of eddies to low oxygen extreme event days in the Atlantic regions is generally smaller. Some areas of the SEA are associated with high percentage contributions (up to ≈ 15%), though the spatial extent of these higher contribution values is less than in the Pacific regions. Finally, there is considerably reduced contribution by CEs and ACEs to low oxygen extreme event days across the NEA region, where both CEs and ACEs are typically only associated with ≈ 2% of total extreme events in a small number of grid cells this region.

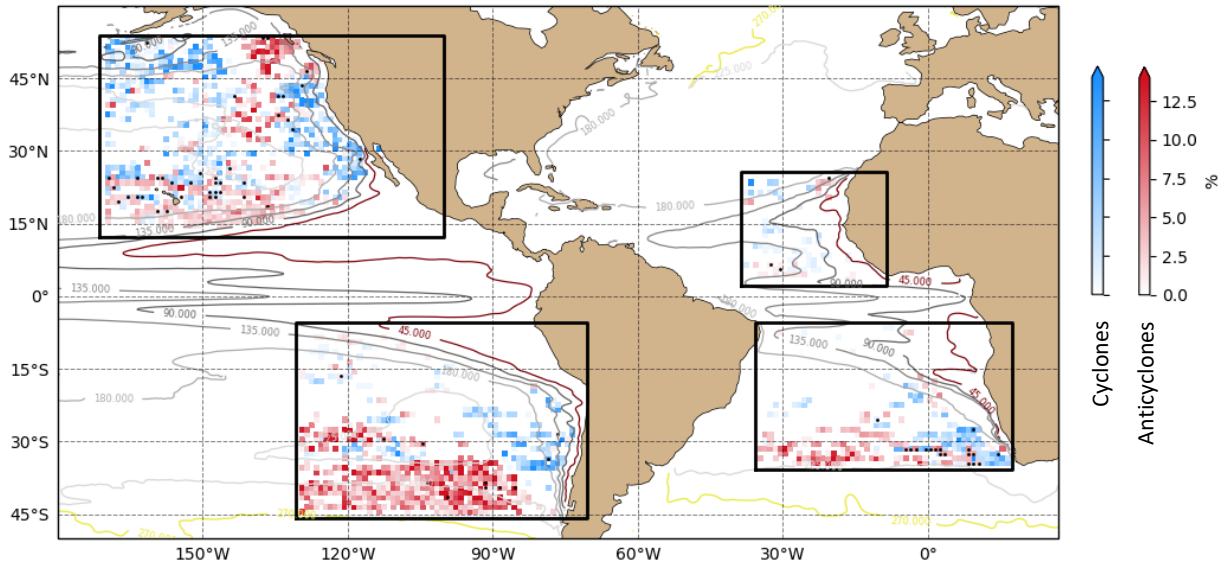

Figure 4.8 – Percentage contribution (% of total number of extreme event days) of low oxygen extreme event days by CEs (blue shading) and ACEs (red shading) in focus regions outside permanent OMZs, across the simulation period 1992-2018, in 1°x1° bins. Only values exceeding 1% are shown. In bins where CEs and ACEs both exceed 1%, the higher value is plotted and stippling marks such locations. Contours show climatological oxygen concentrations (mmol m^{-3}).

5 - Discussion

5.1 – *Eddy-oxygen profiles*

With the advantage of a fully spatiotemporally resolved model dataset, it is shown that mesoscale ocean eddies, especially CEs, significantly influence subsurface oxygen, in surface-visible eddies, in and around global EBUS regions. In Section 4.1, it is shown that eddies propagating across an oxygen gradient (i.e. constrained by an origin in low oxygen waters) have a propensity to contain hypoxic and/or suboxic waters beneath the mixed-layer, in most of this study's focus regions, especially so in comparison to the frequency distributions of climatological oxygen (Figure 4.1). In support of these findings, snap-shot observations of eddies by Karstensen *et al.* (2015) and Schütte *et al.* (2016b) highlight a tendency for severely low oxygen conditions (< 1–10 mmol m^{-3}) to manifest beneath the mixed-layer of CEs and anticyclonic mode-water eddies in the NEA. The eddies tracked in this investigation are shown to be frequently associated with hypoxia (e.g. ≈ 44% of CE cells in the depth range ≈ 50-200 m in the SEA) which is known to promote habitat suppression, and even mortality, of higher trophic level organisms in the ocean (Keeling *et al.*, 2010; Stramma *et al.*, 2012b). Moreover, the relatively frequent association of eddies with suboxia (e.g. ≈ 8% of CE and ACE cells in the depth range 50-200 m in the NEP) demonstrates the capacity of eddies to carry waters potentially conducive to anaerobic metabolisms and production of nitrous oxide, via microbial nitrification and partial denitrification (Vaquer-Sunyer and Duarte, 2008; Codispoti, 2010). A similar effect is demonstrated in Grundle *et al.* (2017), where enhanced nitrous oxide production is observed in low oxygen eddies.

Next, the anomaly fields of oxygen, AOU and O_2sat fields allow us to examine the modulation of the oxygen beneath the mixed-layer by eddies which propagate across the oxygen gradient. The prevalence of strongly negative oxygen anomalies and positive AOU anomalies (Figures 4.2 and 4.3), especially so at depths corresponding approximately to beneath the mixed-layer, indicates low oxygen OMZ source water trapping and eddy-driven oxygen depletion mechanisms by eddies originating in and around the EBUS regions. Eddies which form in the OMZs in the EBUS regions act to 'trap' their low oxygen source waters by virtue of their rotation. That is, strong rotating waters at the eddy circumference prevent the exchange of water mass properties across the eddy boundary (Chelton *et al.*, 2011b). The rotational properties are theorised to be maintained across the eddy lifetime and as they propagate westward. Thus, the water masses contained within the eddy are preserved and display anomalous signals relative to the typically more oxygenated waters found in the areas where eddies are recorded (Frenger *et al.*, 2018). This phenomenon may be applying in CEs and ACEs in this investigation, hence the general tendency here for negative oxygen anomalies in both eddy types in all EBUS regions.

Alongside the trapping of low oxygen source waters, there may be additional eddy-driven oxygen depletion within the eddy structure, as evidenced by enhanced positive AOU anomalies in eddies in Figure 4.3. This is consistent with eddy observational work in the NEA (e.g. Karstensen *et al.*, 2015; Schütte *et al.*, 2016b), where enhanced biological activity is postulated to be a dominant control of oxygen within eddies. Moreover, Gaube *et al.* (2014) show that EBUS regions are generally dominated by areas of negative correlation between SSH and CHL anomaly. Where this negative correlation holds, this implies that surface-depressing (SSH decreasing) CEs are related to positive CHL anomalies (an indicator of biological activity). The results of Gaube *et al.* (2014) therefore match the findings of this investigation where CEs are associated with large anomalies of AOU in and around the EBUS regions. Eddy pumping (e.g. Falkowski *et al.*, 1991) in the early intensification stages of CE lifetimes, or initial trapping of nutrients or organic matter by eddies near the surface from the productive upwelling regions (e.g. Lovecchio *et al.*, 2018) are potential candidate mechanisms for enhanced biological activity within the eddies. Alternatively, mechanisms such as eddy-Ekman pumping, winter mixing, or the combination of both, as proposed in studies such as Dufois *et al.* (2014), Gaube *et al.* (2015) and He *et al.* (2017), may be responsible for enhanced consumption in ACEs shown in this investigation, albeit likely to a weaker degree than the processes in CEs in these focus regions. The findings of this investigation are also consistent with Biogeochemical-Argo float observations of eddies in the North Pacific Subtropical Gyre, where positive AOU anomalies are similarly observed in CEs, and are attributed to enhanced remineralisation of sinking particles (Xiu and Chai, 2020).

5.2 – *Characterisation of low oxygen eddies*

In this investigation, it is noted that eddies of smaller surface radii are associated with greater negative anomalies of oxygen beneath the mixed-layer (Figure 4.5). A proposed explanation could be that smaller radii may lead to increasingly nonlinear (U/c) eddies, as a smaller radius term leads to a greater rotational velocity (U) value if all other variables (e.g. amplitude and translational velocity) remain constant – as expected given Equations 2–5 presented in Section 3.2.2. An increasingly nonlinear eddy may indicate a propensity to preserve a stronger negative oxygen anomaly, whereby enhanced nonlinearity (i.e. $U/c > 1$) indicates rotational velocities (U) which are more likely to exceed translational velocities (c), and as such create a more coherent structure (i.e. Chelton *et al.*, 2011b) capable of trapping low oxygen source waters. However, given the relationships later assessed between eddy rotational velocity/nonlinearity and oxygen anomalies (i.e. Figure 4.6), this explanation is considered less compelling owing to the weak relationships found between those variables.

Alternatively, the cause for the increasingly negative anomalies of oxygen in smaller radius eddies may simply be due to the fact that the oxygen signal is more likely to be concentrated across the smaller volume of a smaller radius eddy. Regardless of the leading mechanism driving the relationship between eddy surface

radius and oxygen anomaly, these findings suggest implications for our understanding of the impact of eddies on the redistribution of oxygen. Namely, they highlight that the results in this investigation may offer a conservative estimate to the redistribution of oxygen in the ocean via eddies, by underestimating the number of strongly deoxygenating eddies. As shown in the physical ocean model validation process (Section 3.3.1), the eddy-permitting resolution model fails to resolve eddies at the lower boundary of the mesoscale (i.e. below ≈ 75 km radius). The ability of a physical ocean model to resolve the mesoscale at different latitudes is governed largely by the ratio between the model horizontal grid spacing and the latitude-dependent Rossby radius of deformation, with the former needing to be significantly lower than the latter for the smallest of mesoscale features to be resolved (Hallberg, 2013; Moreton *et al.*, 2020). This criterion is not always met at eddy-permitting resolution, which leads to an underestimation in the number of smaller eddies resolved. Considering the tendency for stronger deoxygenation in smaller eddies (i.e. Figure 4.5), it is suggested that underestimating the number of smaller eddies in the model also leads to an underestimation of the eddies likely to have the greatest influence on regional oxygen budgets. With increases in model spatial resolution, it is expected that the number of small eddies detected increases (e.g. Moreton *et al.*, 2020), and by extension a better representation the lowest oxygen conditions in the models may also be expected.

5.3 – *Eddy low oxygen extreme events*

In this study, the influence of eddies on low oxygen extreme events is quantified for the first time using novel extreme event metrics. It should be noted that results presented in Section 4.3 – and discussed next – are based on a different constrained eddy dataset to Sections 4.1 and 4.2, as explained in Section 3.2.3. The dataset for Sections 4.1 and 4.2 allows for eddies travelling from a low oxygen origin, across an oxygen gradient into the open ocean to be characterised. Meanwhile, the dataset for Section 4.3 allows for the analysis of eddy contribution to low oxygen extreme events outside of the natural OMZs, without the fixed-percentiles methodology being skewed by permanently low oxygen values. Hence, these constrained datasets are not directly comparable and provide explanation – for example – as to why it is possible for ACEs to demonstrate positive oxygen anomalies in Section 4.1, but exhibit a high frequency of low oxygen extreme events in Section 4.3.

The first evidence of eddy low oxygen extreme event contribution is presented in Figure 4.7, where it is shown that extremely low oxygen conditions inside CEs and/or ACEs are generally more frequent (i.e. > 5% in most focus regions) and more intense (e.g. < 100 mmol m^{-3} in some regions) relative to non-eddying conditions, outside of permanent OMZs. Elzahaby and Schaeffer (2019) show the marked influence of warm-core ACEs on the incidence of marine heatwave events, in the eddy-rich Tasman Sea, with considerable imprints on temperature at depth. This draws parallels to our investigation, where the significant impact of eddies on subsurface oxygen extremes are identified in eddy-rich EBUS focus regions. Finally, in this

investigation strong evidence is presented that both CEs and ACEs contribute substantially (often > 15%) to the number of low oxygen extreme event days, particularly across large areas of the Pacific, outside of permanent OMZs (Figure 4.8). Meanwhile, as demonstrated in Figure 3.2, many areas of the focus regions display peak eddy incidence rates of ≈ 1.5 eddies (which exceed a 1-week lifetime) per year, per 1°x1° bin. This translates to these locations being occupied by eddies for ≈ 0.4% of the temporal extent of the model simulation period. This relatively low percentage incidence of eddies compared to the high percentage contribution values to low oxygen extreme events indicates that eddies act to amplify extremely low oxygen conditions in the focus regions, outside of permanent OMZs.

Localised extremely low oxygen conditions impact marine life and biogeochemistry, and such stressors are typical within permanent OMZs. However, due to the association of low oxygen extreme events and eddies in extra-OMZ locations, it is suggested that eddies act as a vehicle for these stressors to occur outside of OMZs and contribute to a wider distribution of extremely low oxygen conditions in and around EBUS regions. This is similar to suggestions by Frenger *et al.* (2018) who report that simulated subsurface eddies are 'cannonballs' of intensely low oxygen. Observational studies also point towards the ability of such localised pockets of intensely low oxygen concentrations within eddies located in and around EBUS regions to significantly impact marine life and biogeochemistry (e.g. Hauss *et al.*, 2016; Grundle *et al.*, 2017).

6 – Conclusions

6.1 – *Eddies and low oxygen extreme events*

Over the last half-century, ocean deoxygenation (e.g. Schmidtko *et al.*, 2017) and the expansion of OMZs (e.g. Stramma *et al.*, 2012a) has led to increased incidence of low oxygen conditions which are known to negatively impact marine life (e.g. Vaquer-Sunyer and Duarte, 2008; Codispoti, 2010; Keeling *et al.*, 2010). Ocean eddies are mesoscale dynamical features thought to be capable of redistributing oxygen in OMZ regions (Hahn *et al.*, 2014), however a comprehensive, 'complete' dataset analysis of surface-visible eddies and oxygen is lacking. To this end, this study conducts, for the first time, a multi-decadal modelling census of eddies in and around four EBUS focus regions, to assess their position as dynamical vehicles for low oxygen waters and quantify their contribution to low oxygen extreme events in the ocean.

Initial exploration of eddies forming in low oxygen/OMZ regions, and propagating across an oxygen gradient into otherwise more oxygenated waters, shows a propensity for eddies to contain hypoxic and suboxic waters – dissolved oxygen concentrations at which marine life and biogeochemistry are impacted – at depth across most study focus regions. Furthermore, composite eddies in each of the focus regions generally show strong oxygen anomalies beneath the centroids of CEs at a depth range of c 50-200 m, i.e. beneath the mixed layer.

This effect is mirrored by enhanced positive anomalies of AOU beneath the centroids of CEs at the same depth, implying enhanced biological activity as being responsible for a large degree of the oxygen consumption within these eddies. Mechanistic explanations for these findings are postulated to be a combination of physical-biogeochemical processes. For example, the strong rotation of eddies may act to trap source waters upon eddy formation (Chelton *et al.*, 2011b), which are low in oxygen in OMZ regions, whilst vertical movement of nutrients by eddy dynamics (e.g. Falkowski *et al.*, 1991) may cause increased biological activity within eddies.

Next, the defining physical characteristics of a strongly deoxygenating eddy are examined. It is found that surface radius of eddies explains a moderate amount of the variability in oxygen in eddies. That is, smaller radius eddies tend to demonstrate an enhanced negative oxygen anomaly, especially so in CEs. It is postulated that the smaller radius eddies may be resulting in increasingly nonlinear eddies, where rotational velocities exceed translational velocities, and therefore demonstrate enhanced trapping of the low oxygen source waters (Chelton *et al.*, 2011b). However, the relationships examined between rotational velocity vs. oxygen anomaly and nonlinearity vs. oxygen anomaly are weak and do not instil confidence in this being a dominant factor to explain the tendency for the more negatively anomalous oxygen profiles found in eddies with smaller radii. Else, it may be that the low oxygen signals are simply more concentrated across a smaller radius eddy. Regardless of explanation, it is noted that this relationship found between radius and oxygen anomaly should remain an important consideration, given the inability of eddy-permitting models to resolve eddies at the lower boundary of the mesoscale.

In the final section of analysis, the contribution of eddies to low oxygen extreme events outside of OMZs is assessed through a suite of novel extreme event metrics (see Section 3.2.3). That is, the values below the 1st percentile of climatological depth-minimum oxygen. Generally, it is shown that the frequency of low oxygen extreme events is higher in eddies (often ≈ 6-7%) than non-eddying locations (often < 1%), outside of permanent OMZs. Furthermore, there is some evidence of more intense low oxygen extreme events in eddies – especially so in CEs – compared to non-eddies. However, there is increased uncertainty around mean values for this metric. Finally, from a spatial perspective, substantial percentage contributions to the number of low oxygen extreme event days are demonstrated in the Pacific regions, with CEs and ACEs being associated with up to ≈ 15% of extreme events in large areas of the NEP and SEP regions. Atlantic regions show some locations of high percentage contribution (e.g. up to 15% of event days) to low oxygen extreme event days, though to a smaller spatial extent compared to the Pacific regions. These findings hint at the potential for extremely low oxygen conditions to manifest outside of permanent OMZ locations via eddies, therefore highlighting the role of eddies as potential mechanisms for amplifying extreme oxygen conditions in the oceans. This effect may become even more important in more energetic future climate scenarios, given the observed

historical trends of increasing eddy variability in eddy-rich regions under climate warming (e.g. Martínez-Moreno *et al.*, 2021).

6.2 – *Key limitations*

This study is presented as an initial outlook into the interaction between mesoscale ocean eddies and extreme oxygen conditions in the oceans. Despite presenting clear evidence of strongly deoxygenating eddies, there is reason to believe that this investigation still produces a conservative estimate of the contribution of eddies to low oxygen extreme events in and around EBUS regions. Firstly, and as mentioned previously in Section 5.2, it is believed that the lower boundary of the mesoscale (e.g. below ≈ 75 km radius) is not adequately resolved at eddy-permitting resolution (≈ 1/4 °). Secondly, the methodology employed in this investigation, where eddies are identified by their surface SSH signature, means that sub-surface eddies that lack a surface signature – such as the sub-surface intensified eddies examined in Frenger *et al.* (2018) – are not considered here. Thirdly, the eddy tracking algorithm used here – based on Chelton *et al.* (2011b) – is widely applied in other studies, but it does appear to underestimate the number of eddies, especially so in comparison to other methods such as Mason *et al.* (2014) (not shown). With these considerations in mind, it may be that the true number of eddies, and therefore the total contribution of eddies to the extreme state of oxygen in the ocean, is underestimated here. Future work could, therefore, attempt a similar contribution assessment using higher-resolution (e.g. eddy-resolving; 1/12°) simulations and/or different eddy tracking methodologies.

This investigation performs a thorough analysis of eddies and their oxygen signals from climate model data. However, it is still necessarily data limited. That is, this investigation concerns just single member reanalysis simulations – namely the FREEGLORYS2V4 physical model and coupled FREEBIORYS2V4 biogeochemical simulation. In order to gain a greater understanding of the uncertainties associated with the model simulations it is vital to conduct these experiments in multi-model ensemble simulations, where multi-model means can be used to explore the influence of model uncertainty. Regardless, and despite some uncertainty relative to the observations highlighted in Section 3.3.1, the models employed in this study are still considered to skilfully reproduce the structure of OMZs in the EBUS regions (Figure 3.4), as well as key eddy physical characteristics (Figure 3.3). I consider the extreme oxygen anomalies found in the eddies to be valid, though the absolute concentrations may carry a degree of uncertainty. For the reasons outlined above, I aim to frame this work as an attempt towards a 'proof of concept' and a promising outlook into the role that mesoscale eddies have to play in extreme oxygen conditions in the oceans.

References

Aguedjou HMA, Dadou I, Chaigneau A, Morel Y, Alory G. 2019. Eddies in the Tropical Atlantic Ocean and Their Seasonal Variability. *Geophysical Research Letters*, 46(21): 12156–12164. https://doi.org/10.1029/2019GL083925.

Andrews OD, Bindoff NL, Halloran PR, Ilyina T, Le Quéré C. 2013. Detecting an external influence on recent changes in oceanic oxygen using an optimal fingerprinting method. *Biogeosciences*. Copernicus GmbH, 10(3): 1799–1813. https://doi.org/10.5194/bg-10-1799-2013.

Arévalo-Martínez DL, Kock A, Löscher CR, Schmitz RA, Bange HW. 2015. Massive nitrous oxide emissions from the tropical South Pacific Ocean. *Nature Geoscience*. Nature Publishing Group, 8(7): 530–533. https://doi.org/10.1038/ngeo2469.

Arévalo-Martínez DL, Kock A, Löscher CR, Schmitz RA, Stramma L, Bange HW. 2016. Influence of mesoscale eddies on the distribution of nitrous oxide in the eastern tropical South Pacific. *Biogeosciences*. Copernicus GmbH, 13(4): 1105–1118. https://doi.org/10.5194/bg-13-1105-2016.

Arístegui J, Sangrá P, Hernández-León S, Cantón M, Hernández-Guerra A, Kerling JL. 1994. Island-induced eddies in the Canary islands. *Deep Sea Research Part I: Oceanographic Research Papers*, 41(10): 1509–1525. https://doi.org/10.1016/0967-0637(94)90058-2.

Ashkezari MD, Hill CN, Follett CN, Forget G, Follows MJ. 2016. Oceanic eddy detection and lifetime forecast using machine learning methods. *Geophysical Research Letters*, 43(23): 12,234-12,241. https://doi.org/10.1002/2016GL071269.

Aumont O, Ethé C, Tagliabue A, Bopp L, Gehlen M. 2015. PISCES-v2: an ocean biogeochemical model for carbon and ecosystem studies. *Geoscientific Model Development*. Copernicus GmbH, 8(8): 2465–2513. https://doi.org/10.5194/gmd-8-2465-2015.

Berthet S, Séférian R, Bricaud C, Chevallier M, Voldoire A, Ethé C. 2019. Evaluation of an Online Grid-Coarsening Algorithm in a Global Eddy-Admitting Ocean Biogeochemical Model. *Journal of Advances in Modeling Earth Systems*, 11(6): 1759–1783. https://doi.org/10.1029/2019MS001644.

Bopp L, Resplandy L, Orr JC, Doney SC, Dunne JP, Gehlen M, Halloran P, Heinze C, Ilyina T, Séférian R, Tjiputra J, Vichi M. 2013. Multiple stressors of ocean ecosystems in the 21st century: projections with CMIP5 models. *Biogeosciences*. Copernicus GmbH, 10(10): 6225–6245. https://doi.org/10.5194/bg-10-6225-2013.

Bopp L, Resplandy L, Untersee A, Le Mezo P, Kageyama M. 2017. Ocean (de)oxygenation from the Last Glacial Maximum to the twenty-first century: insights from Earth System models. *Philosophical Transactions of the Royal Society A: Mathematical, Physical and Engineering Sciences*. Royal Society, 375(2102): 20160323. https://doi.org/10.1098/rsta.2016.0323.

Cabré A, Marinov I, Bernardello R, Bianchi D. 2015. Oxygen minimum zones in the tropical Pacific across CMIP5 models: mean state differences and climate change trends. *Biogeosciences*. Copernicus GmbH, 12(18): 5429–5454. https://doi.org/10.5194/bg-12-5429-2015.

Chaigneau A, Eldin G, Dewitte B. 2009. Eddy activity in the four major upwelling systems from satellite altimetry (1992–2007). *Progress in Oceanography*, 83(1): 117–123. https://doi.org/10.1016/j.pocean.2009.07.012.

Chaigneau A, Gizolme A, Grados C. 2008. Mesoscale eddies off Peru in altimeter records: Identification algorithms and eddy spatio-temporal patterns. *Progress in Oceanography*, 79(2): 106–119. https://doi.org/10.1016/j.pocean.2008.10.013.

Chaigneau A, Pizarro O. 2005. Eddy characteristics in the eastern South Pacific. *Journal of Geophysical Research: Oceans*, 110(C6). https://doi.org/10.1029/2004JC002815.

Chelton DB, Gaube P, Schlax MG, Early JJ, Samelson RM. 2011a. The influence of nonlinear mesoscale eddies on near-surface oceanic chlorophyll. *Science (New York, NY)*, 334(6054): 328–332. https://doi.org/10.1126/science.1208897.

Chelton DB, Schlax MG. 1996. Global Observations of Oceanic Rossby Waves. *Science*. American Association for the Advancement of Science, 272(5259): 234–238. https://doi.org/10.1126/science.272.5259.234.

Chelton DB, Schlax MG. 2016. The “growing method” of Eddy identification and tracking in two and three dimensions. Corvallis, OR, Oregon State University: College of Earth, Ocean and Atmospheric Sciences.

Chelton DB, Schlax MG, Freilich MH, Milliff RF. 2004. Satellite Measurements Reveal Persistent Small-Scale Features in Ocean Winds. *Science*. American Association for the Advancement of Science, 303(5660): 978–983. https://doi.org/10.1126/science.1091901.

Chelton DB, Schlax MG, Samelson RM. 2011b. Global observations of nonlinear mesoscale eddies. *Progress in Oceanography*, 91(2): 167–216. https://doi.org/10.1016/j.pocean.2011.01.002.

Chelton DB, Schlax MG, Samelson RM, Szoeke RA de. 2007. Global observations of large oceanic eddies. *Geophysical Research Letters*, 34(15). https://doi.org/10.1029/2007GL030812.

Codispoti LA. 2010. Interesting Times for Marine N2O. *Science*. American Association for the Advancement of Science, 327(5971): 1339–1340. https://doi.org/10.1126/science.1184945.

Czeschel R, Schütte F, Weller RA, Stramma L. 2018. Transport, properties, and life cycles of mesoscale eddies in the eastern tropical South Pacific. *Ocean Science*. Copernicus GmbH, 14(4): 731–750. https://doi.org/10.5194/os-14-731-2018.

Deremble B, Dewar WK, Chassignet EP. 2016. Vorticity dynamics near sharp topographic features. *Journal of Marine Research*, 74(6): 249–276. https://doi.org/10.1357/002224016821744142.

Diaz RJ, Rosenberg R. 2008. Spreading dead zones and consequences for marine ecosystems. *Science (New York, NY)*, 321(5891): 926–929. https://doi.org/10.1126/science.1156401.

Djakouré S, Penven P, Bourlès B, Veitch J, Koné V. 2014. Coastally trapped eddies in the north of the Gulf of Guinea. *Journal of Geophysical Research: Oceans*, 119(10): 6805–6819. https://doi.org/10.1002/2014JC010243.

Dufois F, Hardman-Mountford NJ, Greenwood J, Richardson AJ, Feng M, Herbette S, Matear R. 2014. Impact of eddies on surface chlorophyll in the South Indian Ocean. *Journal of Geophysical Research: Oceans*, 119(11): 8061–8077. https://doi.org/10.1002/2014JC010164.

Dufois F, Hardman-Mountford NJ, Greenwood J, Richardson AJ, Feng M, Matear RJ. 2016. Anticyclonic eddies are more productive than cyclonic eddies in subtropical gyres because of winter mixing. *Science Advances*, 2(5). https://doi.org/10.1126/sciadv.1600282.

Elzahaby Y, Schaeffer A. 2019. Observational Insight Into the Subsurface Anomalies of Marine Heatwaves. *Frontiers in Marine Science*. Frontiers, 6. https://doi.org/10.3389/fmars.2019.00745.

Everett JD, Baird ME, Oke PR, Suthers IM. 2012. An avenue of eddies: Quantifying the biophysical properties of mesoscale eddies in the Tasman Sea. *Geophysical Research Letters*, 39(16). https://doi.org/10.1029/2012GL053091.

Faghmous JH, Frenger I, Yao Y, Warmka R, Lindell A, Kumar V. 2015. A daily global mesoscale ocean eddy dataset from satellite altimetry. *Scientific Data*. Nature Publishing Group, 2(1): 150028. https://doi.org/10.1038/sdata.2015.28.

Falkowski PG, Ziemann D, Kolber Z, Bienfang PK. 1991. Role of eddy pumping in enhancing primary production in the ocean. *Nature*. Nature Publishing Group, 352(6330): 55–58. https://doi.org/10.1038/352055a0.

Fang F, Morrow R. 2003. Evolution, movement and decay of warm-core Leeuwin Current eddies. *Deep Sea Research Part II: Topical Studies in Oceanography*, 50(12): 2245–2261. https://doi.org/10.1016/S0967-0645(03)00055-9.

Farías L, Castro-González M, Cornejo M, Charpentier J, Faúndez J, Boontanon N, Yoshida N. 2009. Denitrification and nitrous oxide cycling within the upper oxycline of the eastern tropical South Pacific oxygen minimum zone. *Limnology and Oceanography*, 54(1): 132–144. https://doi.org/10.4319/lo.2009.54.1.0132.

Fiedler B, Grundle DS, Schütte F, Karstensen J, Löscher CR, Hauss H, Wagner H, Loginova A, Kiko R, Silva P, Tanhua T, Körtzinger A. 2016. Oxygen utilization and downward carbon flux in an oxygen-depleted eddy in the eastern tropical North Atlantic. *Biogeosciences*. Copernicus GmbH, 13(19): 5633–5647. https://doi.org/10.5194/bg-13-5633-2016.

Flierl GR, McGillicuddy DJ. 2002. Mesoscale and submesoscale physical-biological interactions. *The Sea*. Wiley & Sons: New York, NY, 113–185.

Fox-Kemper B, Bachman S, Pearson B, S. Reckinger. 2014. Principles and advances in subgrid modeling for eddy-rich simulations. *CLIVAR Exchanges: Special Issue: High Resolution Ocean Climate Modelling*, 19(65).

Frenger I, Bianchi D, Stührenberg C, Oschlies A, Dunne J, Deutsch C, Galbraith E, Schütte F. 2018. Biogeochemical Role of Subsurface Coherent Eddies in the Ocean: Tracer Cannonballs, Hypoxic Storms, and Microbial Stewpots? *Global Biogeochemical Cycles*, 32(2): 226–249. https://doi.org/10.1002/2017GB005743.

Frölicher TL, Fischer EM, Gruber N. 2018. Marine heatwaves under global warming. *Nature*. Nature Publishing Group, 560(7718): 360–364. https://doi.org/10.1038/s41586-018-0383-9.

Garcia H, Weathers K, Paver C, Smolyar I, Boyer T, Locarnini R, Zweng M, Mishonov A, Baranova O, Seidov D, Reagan J. 2019a. World Ocean Atlas 2018 Volume 3: Dissolved Oxygen, Apparent Oxygen Utilization, and Dissolved Oxygen Saturation. NOAA Atlas NESDIS.

Garcia H, Weathers K, Paver C, Smolyar I, Boyer T, Locarnini R, Zweng M, Mishonov A, Baranova O, Seidov D, Reagan J, Grodsky C. 2019b. World Ocean Atlas 2018: Product Documentation. Mishonov A, Technical Editor.

Gaube P, Chelton DB, Samelson RM, Schlax MG, O'Neill LW. 2015. Satellite Observations of Mesoscale Eddy-Induced Ekman Pumping. *Journal of Physical Oceanography*. American Meteorological Society, 45(1): 104–132. https://doi.org/10.1175/JPO-D-14-0032.1.

Gaube P, Chelton DB, Strutton PG, Behrenfeld MJ. 2013. Satellite observations of chlorophyll, phytoplankton biomass, and Ekman pumping in nonlinear mesoscale eddies. *Journal of Geophysical Research: Oceans*, 118(12): 6349–6370. https://doi.org/10.1002/2013JC009027.

Gaube P, McGillicuddy DJ, Chelton DB, Behrenfeld MJ, Strutton PG. 2014. Regional variations in the influence of mesoscale eddies on near-surface chlorophyll. *Journal of Geophysical Research: Oceans*, 119(12): 8195–8220. https://doi.org/10.1002/2014JC010111.

Gaube P, McGillicuddy DJ, Moulin AJ. 2019. Mesoscale Eddies Modulate Mixed Layer Depth Globally. *Geophysical Research Letters*, 46(3): 1505–1512. https://doi.org/10.1029/2018GL080006.

Gray J, Wu R, Or Y. 2002. Effects of hypoxia and organic enrichment on the coastal marine environment. *Marine Ecology-Progress Series*, 238: 249–279. https://doi.org/10.3354/meps238249.

Greenwood JE, Feng M, Waite AM. 2007. A one-dimensional simulation of biological production in two contrasting mesoscale eddies in the south eastern Indian Ocean. *Deep Sea Research Part II: Topical Studies in Oceanography*, 54(8): 1029–1044. https://doi.org/10.1016/j.dsr2.2006.10.004.

Gruber N. 2008. The Marine Nitrogen Cycle: Overview and Challenges. *Nitrogen in the Marine Environment*, Academic Press: New York, NY, 1–50.

Grundle DS, Löscher CR, Krahmann G, Altabet MA, Bange HW, Karstensen J, Körtzinger A, Fiedler B. 2017. Low oxygen eddies in the eastern tropical North Atlantic: Implications for N 2 O cycling. *Scientific Reports*. Nature Publishing Group, 7(1): 4806. https://doi.org/10.1038/s41598-017-04745-y.

Hahn J, Brandt P, Greatbatch RJ, Krahmann G, Körtzinger A. 2014. Oxygen variance and meridional oxygen supply in the Tropical North East Atlantic oxygen minimum zone. *Climate Dynamics*, 43(11): 2999–3024. https://doi.org/10.1007/s00382-014-2065-0.

Hallberg R. 2013. Using a resolution function to regulate parameterizations of oceanic mesoscale eddy effects. *Ocean Modelling*, 72: 92–103. https://doi.org/10.1016/j.ocemod.2013.08.007.

Halo I, Backeberg B, Penven P, Ansorge I, Reason C, Ullgren JE. 2014. Eddy properties in the Mozambique Channel: A comparison between observations and two numerical ocean circulation models. *Deep Sea Research Part II: Topical Studies in Oceanography*, 100: 38–53. https://doi.org/10.1016/j.dsr2.2013.10.015.

Hauss H, Christiansen S, Schütte F, Kiko R, Edvam Lima M, Rodrigues E, Karstensen J, Löscher CR, Körtzinger A, Fiedler B. 2016. Dead zone or oasis in the open ocean? Zooplankton distribution and migration in low-oxygen modewater eddies. *Biogeosciences*. Copernicus GmbH, 13(6): 1977–1989. https://doi.org/10.5194/bg-13-1977-2016.

He Q, Zhan H, Cai S, Zha G. 2016. On the asymmetry of eddy-induced surface chlorophyll anomalies in the southeastern Pacific: The role of eddy-Ekman pumping. *Progress in Oceanography*, 141: 202–211. https://doi.org/10.1016/j.pocean.2015.12.012.

He Q, Zhan H, Shuai Y, Cai S, Li QP, Huang G, Li J. 2017. Phytoplankton bloom triggered by an anticyclonic eddy: The combined effect of eddy-Ekman pumping and winter mixing. *Journal of Geophysical Research: Oceans*, 122(6): 4886–4901. https://doi.org/10.1002/2017JC012763.

Hewitt HT, Bell MJ, Chassignet EP, Czaja A, Ferreira D, Griffies SM, Hyder P, McClean JL, New AL, Roberts MJ. 2017. Will high-resolution global ocean models benefit coupled predictions on short-range to climate timescales? *Ocean Modelling*, 120: 120–136. https://doi.org/10.1016/j.ocemod.2017.11.002.

Hewitt HT, Roberts M, Mathiot P, Biastoch A, Blockley E, Chassignet EP, Fox-Kemper B, Hyder P, Marshall DP, Popova E, Treguier A-M, Zanna L, Yool A, Yu Y, Beadling R, Bell M, Kuhlbrodt T, Arsouze T, Bellucci A, Castruccio F, Gan B, Putrasahan D, Roberts CD, Van Roekel L, Zhang Q. 2020. Resolving and Parameterising the Ocean Mesoscale in Earth System Models. *Current Climate Change Reports*. https://doi.org/10.1007/s40641-020-00164-w.

Isern-Fontanet J, García-Ladona E, Font J. 2003. Identification of Marine Eddies from Altimetric Maps. *Journal of Atmospheric and Oceanic Technology*. American Meteorological Society, 20(5): 772–778. https://doi.org/10.1175/1520-0426(2003)20<772:IOMEFA>2.0.CO;2.

Jansen MF, Held IM. 2014. Parameterizing subgrid-scale eddy effects using energetically consistent backscatter. *Ocean Modelling*, 80: 36–48. https://doi.org/10.1016/j.ocemod.2014.06.002.

Karstensen J, Fiedler B, Schütte F, Brandt P, Arne K, Fischer G, Visbeck M, Zantopp R, Hahn J, Wallace DWR. 2015. Open ocean dead zones in the tropical North Atlantic Ocean. *Biogeosciences*, 12: 2597–2605. https://doi.org/10.5194/bg-12-2597-2015.

Karstensen J, Stramma L, Visbeck M. 2008. Oxygen minimum zones in the eastern tropical Atlantic and Pacific oceans. *Progress in Oceanography*, 77(4): 331–350. https://doi.org/10.1016/j.pocean.2007.05.009.

Keeling RF, Körtzinger A, Gruber N. 2010. Ocean Deoxygenation in a Warming World. *Annual Review of Marine Science*, 2(1): 199–229. https://doi.org/10.1146/annurev.marine.010908.163855.

Klein P, Lapeyre G. 2009. The Oceanic Vertical Pump Induced by Mesoscale and Submesoscale Turbulence. *Annual Review of Marine Science*, 1(1): 351–375. https://doi.org/10.1146/annurev.marine.010908.163704.

Kostianoy A, Belkin I. 1989. A Survey of Observations on Intrathermocline Eddies in the World Ocean. *Elsevier Oceanography Series*, 821–841.

Löscher CR, Fischer MA, Neulinger SC, Fiedler B, Philippi M, Schütte F, Singh A, Hauss H, Karstensen J, Körtzinger A, Künzel S, Schmitz RA. 2015. Hidden biosphere in an oxygen-deficient Atlantic open-ocean eddy: future implications of ocean deoxygenation on primary production in the eastern tropical North Atlantic. *Biogeosciences*. Copernicus GmbH, 12(24): 7467–7482. https://doi.org/10.5194/bg-12-7467-2015.

Lovecchio E, Gruber N, Münnich M. 2018. Mesoscale contribution to the long-range offshore transport of organic carbon from the Canary Upwelling System to the open North Atlantic. *Biogeosciences*. Copernicus GmbH, 15(16): 5061–5091. https://doi.org/10.5194/bg-15-5061-2018.

Madec G. 2008. NEMO Ocean Engine, Note du Pole de Modelisation. Institut Pierre-Simon Laplace (IPSL): Paris, FR.

Mahadevan A. 2014. Eddy effects on biogeochemistry. *Nature*. Nature Publishing Group, 506(7487): 168–169. https://doi.org/10.1038/nature13048.

Martínez-Moreno J, Hogg AM, England MH, Constantinou NC, Kiss AE, Morrison AK. 2021. Global changes in oceanic mesoscale currents over the satellite altimetry record. *Nature Climate Change*. Nature Publishing Group, 11(5): 397–403. https://doi.org/10.1038/s41558-021-01006-9.

Mason E, Pascual A, McWilliams JC. 2014. A New Sea Surface Height–Based Code for Oceanic Mesoscale Eddy Tracking. *Journal of Atmospheric and Oceanic Technology*. American Meteorological Society, 31(5): 1181–1188. https://doi.org/10.1175/JTECH-D-14-00019.1.

Matear RJ, Chamberlain MA, Sun C, Feng M. 2013. Climate change projection of the Tasman Sea from an Eddy-resolving Ocean Model. *Journal of Geophysical Research: Oceans*, 118(6): 2961–2976. https://doi.org/10.1002/jgrc.20202.

McGillicuddy DJ. 2016. Mechanisms of Physical-Biological-Biogeochemical Interaction at the Oceanic Mesoscale. *Annual Review of Marine Science*, 8(1): 125–159. https://doi.org/10.1146/annurev-marine-010814-015606.

McWilliams JC. 2006. *Fundamentals of Geophysical Fluid Dynamics*. Cambridge University Press: Cambridge.

Menkes CE, Kennan SC, Flament P, Dandonneau Y, Masson S, Biessy B, Marchal E, Eldin G, Grelet J, Montel Y, Morlière A, Lebourges-Dhaussy A, Moulin C, Champalbert G, Herbland A. 2002. A whirling ecosystem in the equatorial Atlantic. *Geophysical Research Letters*, 29(11): 48-1-48–4. https://doi.org/10.1029/2001GL014576.

Moore TS, Matear RJ, Marra J, Clementson L. 2007. Phytoplankton variability off the Western Australian Coast: Mesoscale eddies and their role in cross-shelf exchange. *Deep Sea Research Part II: Topical Studies in Oceanography*, 54(8): 943–960. https://doi.org/10.1016/j.dsr2.2007.02.006.

Moreton SM, Ferreira D, Roberts MJ, Hewitt HT. 2020. Evaluating surface eddy properties in coupled climate simulations with 'eddy-present' and 'eddy-rich' ocean resolution. *Ocean Modelling*, 147: 101567. https://doi.org/10.1016/j.ocemod.2020.101567.

Morrow R, Birol F, Griffin D, Sudre J. 2004. Divergent pathways of cyclonic and anti-cyclonic ocean eddies. *Geophysical Research Letters*, 31(24). https://doi.org/10.1029/2004GL020974.

Müller V. 2017. Temperature and Freshwater Fluxes by Individual Eddies in North Atlantic Ocean. Dr. rer. nat., Universität Bremen.

Naqvi SWA, Bange HW, Farías L, Monteiro PMS, Scranton MI, Zhang J. 2010. Marine hypoxia/anoxia as a source of CH_4 and N_2O. *Biogeosciences*. Copernicus GmbH, 7(7): 2159–2190. https://doi.org/10.5194/bg-7-2159-2010.

Olbers D, Willebrand J, Eden C. 2012. *Ocean Dynamics*. Springer Science & Business Media: Berlin Heidelberg, DE.

Oliver ECJ, Burrows MT, Donat MG, Sen Gupta A, Alexander LV, Perkins-Kirkpatrick SE, Benthuysen JA, Hobday AJ, Holbrook NJ, Moore PJ, Thomsen MS, Wernberg T, Smale DA. 2019. Projected Marine Heatwaves in the 21st Century and the Potential for Ecological Impact. *Frontiers in Marine Science*. Frontiers, 6. https://doi.org/10.3389/fmars.2019.00734.

Oliver ECJ, O'Kane TJ, Holbrook NJ. 2015. Projected changes to Tasman Sea eddies in a future climate. *Journal of Geophysical Research: Oceans*, 120(11): 7150–7165. https://doi.org/10.1002/2015JC010993.

Oschlies A, Brandt P, Stramma L, Schmidtko S. 2018. Drivers and mechanisms of ocean deoxygenation. *Nature Geoscience*. Nature Publishing Group, 11(7): 467–473. https://doi.org/10.1038/s41561-018-0152-2.

Paulmier A, Ruiz-Pino D. 2009. Oxygen minimum zones (OMZs) in the modern ocean. *Progress in Oceanography*, 80(3): 113–128. https://doi.org/10.1016/j.pocean.2008.08.001.

Penven P, Echevin V, Pasapera J, Colas F, Tam J. 2005. Average circulation, seasonal cycle, and mesoscale dynamics of the Peru Current System: A modeling approach. *Journal of Geophysical Research: Oceans*, 110(C10). https://doi.org/10.1029/2005JC002945.

Perruche C, Szczypta C, Paul J, Drévillon M. 2019. Quality Information Document - GLOBAL_REANALYSIS_BIO_001_029. Copernicus Marine Environment Monitoring Service.

Pujol M-I, Mertz F. 2020. Global Ocean Gridded L4 Sea Surface Heights and Derived Varaibles NRT - Product User Manual. Copernicus Marine Environment Monitoring Service.

Rhein M, Rintoul S, Aoki S, Campos E, Chambers D, Feely R, Gulev S, Johnson G, Josey S, Kostianoy A, Mauritzen C, Roemmich D, Talley L, Wang F. 2013. Observations: ocean. *Climate Change 2013: The Physical Science Basis. Contribution of Working Group I to the Fifth Assessment Report of the Intergovernmental Panel on Climate Change [Stocker, T.F., D. Qin, G.-K. Plattner, M. Tignor, S.K. Allen, J. Boschung, A. Nauels, Y. Xia, V. Bex and P.M. Midgley (eds.)]*. Cambridge University Press: Cambridge, UK.

Rhines PB. 2001. Mesoscale Eddies. *Encyclopedia of Ocean Sciences*. Academic Press: Oxford, 755–767.

Rossby C-G, Collaborators. 1939. Relations between variations in the intensity of the zonal circulationof the atmosphere and the displacements of the semipermantent centers of action. *Journal of Marine Research*, 2: 38–55.

Rykova T, Oke PR. 2015. Recent freshening of the East Australian Current and its eddies. *Geophysical Research Letters*, 42(21): 9369–9378. https://doi.org/10.1002/2015GL066050.

Schmidtko S, Stramma L, Visbeck M. 2017. Decline in global oceanic oxygen content during the past five decades. *Nature*. Nature Publishing Group, 542(7641): 335–339. https://doi.org/10.1038/nature21399.

Schütte F, Brandt P, Karstensen J. 2016a. Occurrence and characteristics of mesoscale eddies in the tropical northeastern Atlantic Ocean. *Ocean Science*. Copernicus GmbH, 12(3): 663–685. https://doi.org/10.5194/os-12-663-2016.

Schütte F, Karstensen J, Krahmann G, Hauss H, Fiedler B, Brandt P, Visbeck M, Körtzinger A. 2016b. Characterization of “dead-zone” eddies in the eastern tropical North Atlantic. *Biogeosciences*. Copernicus GmbH, 13(20): 5865–5881. https://doi.org/10.5194/bg-13-5865-2016.

Séférian R, Berthet S, Yool A, Palmiéri J, Bopp L, Tagliabue A, Kwiatkowski L, Aumont O, Christian J, Dunne J, Gehlen M, Ilyina T, John JG, Li H, Long MC, Luo JY, Nakano H, Romanou A, Schwinger J, Stock C, Santana-Falcón Y, Takano Y, Tjiputra J, Tsujino H, Watanabe M, Wu T, Wu F, Yamamoto A. 2020. Tracking Improvement in Simulated Marine Biogeochemistry Between CMIP5 and CMIP6. *Current Climate Change Reports*, 6(3): 95–119. https://doi.org/10.1007/s40641-020-00160-0.

Stramma L, Bange HW, Czeschel R, Lorenzo A, Frank M. 2013. On the role of mesoscale eddies for the biological productivity and biogeochemistry in the eastern tropical Pacific Ocean off Peru. *Biogeosciences*, 10: 7293–7306. https://doi.org/10.5194/bg-10-7293-2013.

Stramma L, Oschlies A, Schmidtko S. 2012a. Mismatch between observed and modeled trends in dissolved upper-ocean oxygen over the last 50 yr. *Biogeosciences*. Copernicus GmbH, 9(10): 4045–4057. https://doi.org/10.5194/bg-9-4045-2012.

Stramma L, Prince ED, Schmidtko S, Luo J, Hoolihan JP, Visbeck M, Wallace DWR, Brandt P, Körtzinger A. 2012b. Expansion of oxygen minimum zones may reduce available habitat for tropical pelagic fishes. *Nature Climate Change*. Nature Publishing Group, 2(1): 33–37. https://doi.org/10.1038/nclimate1304.

Vallis GK. 2017. *Atmospheric and Oceanic Fluid Dynamics: Fundamentals and Large-Scale Circulation*. Cambridge University Press: Cambridge.

Vaquer-Sunyer R, Duarte CM. 2008. Thresholds of hypoxia for marine biodiversity. *Proceedings of the National Academy of Sciences*. National Academy of Sciences, 105(40): 15452–15457. https://doi.org/10.1073/pnas.0803833105.

Waite AM, Pesant S, Griffin DA, Thompson PA, Holl CM. 2007. Oceanography, primary production and dissolved inorganic nitrogen uptake in two Leeuwin Current eddies. *Deep Sea Research Part II: Topical Studies in Oceanography*, 54(8): 981–1002. https://doi.org/10.1016/j.dsr2.2007.03.001.

Weiss RF. 1970. The solubility of nitrogen, oxygen and argon in water and seawater. *Deep Sea Research and Oceanographic Abstracts*, 17(4): 721–735. https://doi.org/10.1016/0011-7471(70)90037-9.

Xiu P, Chai F. 2020. Eddies Affect Subsurface Phytoplankton and Oxygen Distributions in the North Pacific Subtropical Gyre. *Geophysical Research Letters*, 47(15): e2020GL087037. https://doi.org/10.1029/2020GL087037.

Zhang Y, Tian F, Ge C. 2016. Characteristics of Global Oceanic Rossby Wave and Mesoscale Eddies Propagation from Multiple Datasets Analysis. *Ocean Science Discussions*, 1–26. https://doi.org/10.5194/os-2016-64.